[Cell Cycle 3:6, 722-724; June 2004]; ©2004 Landes Bioscience

Extra Views

Runx1/AML-1 Ranks as a Master Regulator of Adult Hematopoiesis

Motoshi Ichikawa
Takashi Asai
Shigeru Chiba
Mineo Kurokawa
Seishi Ogawa*

Department of Hematology and Oncology; Graduate School of Medicine; University of Tokyo; Tokyo, Japan

*Correspondence to: Seishi Ogawa; Department of Hematology and Oncology; Graduate School of Medicine; University of Tokyo; Tokyo 113-8655 Japan; Tel.: +81.3.3815.5411x30673; Fax: +81.3.5804.6261; Email: sogawa-tky@umin.ac.jp

Received 04/27/04; Accepted04/28/04

Previously published online as a *Cell Cycle* E-publication:
http://www.landesbioscience.com/journals/cc/abstract.php?id=951

KEY WORDS

Runx1, hematopoietic stem cells, platelets, leukemogenesis, transcription factors

ACKNOWLEDGEMENTS

We are deeply indebted to the late Dr. Hisamaru Hirai for the works on which the essential part of this review is based and also for his great leadership in our laboratory, which was abruptly terminated by his unexpected death on August 23, 2003. We would like to dedicate this review to the memory of our beloved friend.

ABSTRACT

Runx1 (AML-1) is a critical gene involved in human leukemogenesis, originally identified at the 21q22 breakpoint of the leukemic translocations of t(8;21)(q21;q22), and is thought to be involved in as much as 25% of human leukemia. It encodes a transcription factor that has close homology to a *Drosophila* protein, runt, and is found to play essential roles in regulation of hematopoietic systems. Really a gene disruption experiment unequivocally shows that Runx1 is absolutely required for the establishment of definitive or adult-type hematopoiesis. Moreover, accumulated evidence from a number of in vitro studies and findings in patients with familial platelet disorder with predisposition to acute myelogenous leukemia (FPD/AML) strongly suggests that it also commits to the control of hematopoietic system in adult life, although the in depth analysis of its roles in adult hematopoiesis has been largely hampered by premature lethality of *Runx1*-null animals. Recently we have developed conditional knockout mice in which *Runx1* is disrupted specifically in hematopoietic compartments after birth and dissected its roles in adult hematopoiesis. Notably, in these mice, maturation of megakaryocytes and development of both T and B lymphocytes were severely impaired, whereas hematopoietic progenitors were maintained or even expanded with apparently normal myeloid and erythroid differentiation in the periphery and bone marrow. Our findings clearly demonstrated differential requirement of *Runx1* in stem cell development and in its maintenance together with multi-modal functions of this transcription factor that are critically required for maturation of megakaryocytes and lymphocyte development, also providing a novel insight into how deeply and meticulously Runx1 is involved in regulation of mammalian hematopoiesis.

Mammalian hematopoietic development is believed to arise from two distinct cellular origins. In mice, the primitive erythroid cells that appears around day 7.5 postcoitus (E7.5) in the yolk sac is the first hematopoiesis thus far detected, known as primitive hematopoiesis, and is exclusively composed of large and nucleated erythrocytes.[1] On the other hand, the second wave of hematopoiesis, or definitive hematopoiesis, is heralded later in the ventral region of the aorta-gonad-mesonephros (AGM) region in E10.5 and consists of enucleated erythrocytes, myeloid cells and lymphoid progenitors, which ensures following expansion of hematopoietic stem cells (HSCs) and blood production in the fetal liver around E12.5.[2] These are finely regulated processes in which a bunch of genes are expressed in a well-coordinated manner and the growing lines of evidence suggest that these regulations are mediated by a number of hematopoietic transcription factors.

Runx1, also known as *AML-1*, *CBFA2* or *PEBP2αB* is a transcription factor first isolated from t(8;21)(q21;q22) and later in t(3;21)(q26;q22), t(12;21)(p13;q22), and t(16;21)(q24;q21) translocations found in human leukemia in which the aberrant fusion genes, *AML-1/ETO* and *AML-1/Evi1*, *TEL/AML-1*, and *AML-1/MTG16*, were generated, respectively.[3] It has high homology to the *Drosophila* segmentation gene, *runt*, and also has two mammalian homologues, Runx2 (AML-3) and Runx3 (AML-2), collectively called the *Runx* family transcription factors. It is shown that Runx1 dimerizes with the common β-subunit, CBFβ, to bind to its target sequences known as PEBP2 sequences and regulates a variety of hematopoietic lineage-specific genes, including interleukin-3, granulocyte-macrophage colony stimulating factor, macrophage colony stimulating factor receptor, neutrophil elastase, granzyme B, myeloperoxidase, neutrophil defensin, and subunits of the T-cell and B-cell antigen receptor, in cooperation with other transcription factors.[3] Runx1 is absolutely required for mouse embryogenesis and hematopoiesis, since *Runx1*-null embryos die at midgestation by E12.5 with massive hemorrhage in the central nervous system and complete effacement of definitive hematopoiesis in the fetal liver, though primitive erythropoiesis is preserved.[4,5] In fact it has been demonstrated using

Runx1-LacZ knock-in embryos that Runx1 is essential for development of HSCs from the endothelial cells in the embryonic AGM region,[6] where definitive hematopoiesis specifically arises from the ventral endothelial linings that express Runx1.

On the other hand, genetic analysis of Runx1 functions in adult life is largely limited because of the embryonic lethality of the homozygously gene-targeted mice, and our knowledge about its in vivo functions in adult hematopoiesis has mostly come from the analysis of murine models of *Runx1*-involving translocations, although there exist a large body of in vitro studies that argue its postnatal functions. Among these, the most intensively studied is *AML-1-ETO* generated in t(8;21)(q21;q22) translocation. Since this aberrant Runx1 (AML-1) fusion protein seems to have a dominant-negative effect on Runx1 functions and its knock-in mice recapitulate a *Runx1*-null phenotype, several mice models of t(8;21)(q21;q22) have been developed using inducible or retrovirus-mediated expression of the fusion protein in bone marrow in order to clarify its leukemogenic functions in vivo.[7-9] The common features of these mouse models are expanded hematopoietic progenitor pools and increased self-renewal capacity of stem cells with varying degrees of abnormalities in differentiation. While these observations provide important clues to the understanding of leukemogenic mechanism through AML-1-ETO and also of physiological Runx1 functions, it cannot be determined to what extent we are able to ascribe these phenotypes to loss of Runx1 functions.

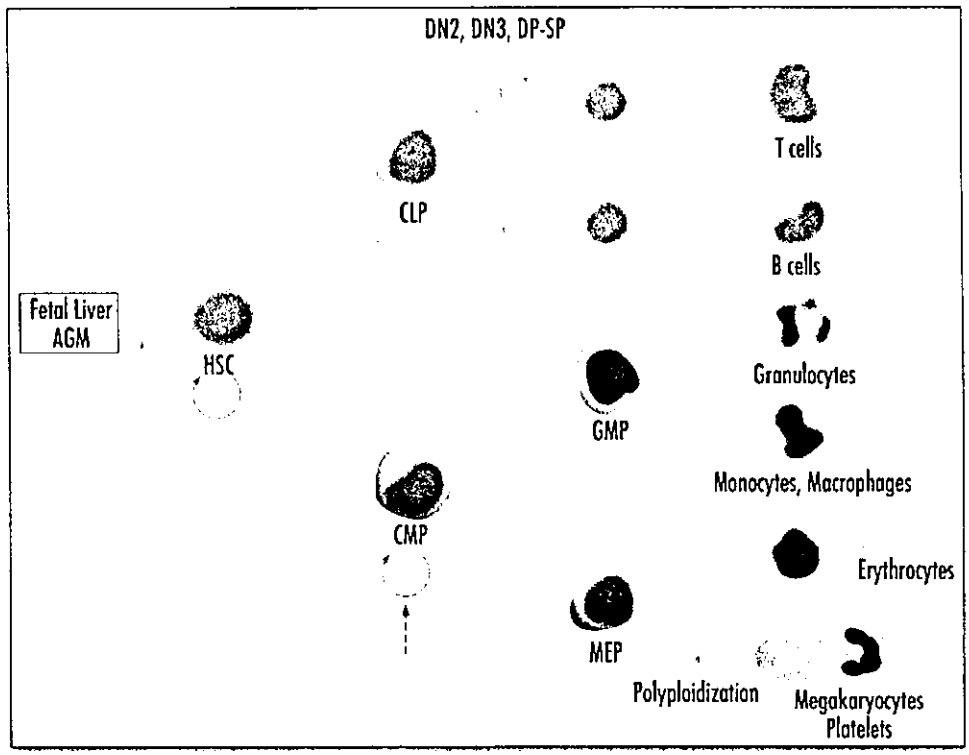

Figure 1. Function of Runx1 in adult hematopoietic maintenance. Red arrows: Runx1 is required. Runx1 is required for development of definitive hematopoiesis at the embryonic stage, several steps in T cell development, early B cell development, and polyploidization of the megakaryocytes, but not for maintenance of early hematopoietic progenitors. Runx1 also negatively regulates the number of myeloid progenitors (broken arrow).

In the article recently published, we analyzed the in vivo role of Runx1 in adult hematopoiesis using the conditional gene targeting system.[10] We generated mice in which exon 5 of the *Runx1* locus was flanked by two *loxP* sites and bred them with mice expressing an interferon-inducible Cre recombinase. With this approach, *Runx1* could be successfully disrupted in the hematopoietic compartments in the adult animals. Although the absence of *Runx1* during developmental stages results in total loss of definitive hematopoiesis and HSC generation, in our conditional knockout mice hematopoietic progenitors were maintained with normal myeloid as well as erythroid development despite complete lack of Runx1, demonstrating that Runx1 is not absolutely required for the maintenance of established adult HSCs per se. It was further supported by transplantation experiments of *Runx1*-null bone marrow cells, in which *Runx1*-null hematopoietic progenitors could fully repopulate recipients' bone marrow for at least three months. On the other hand, however, there exist severe defects about *Runx1*-null hematopoietic progenitors in producing platelets and mature lymphocytes.

A number of transcription factors, including c-Myb, GATA-1, GATA-2, SCL, and LMO-2, also participate in the regulation of the committed hematopoietic progenitors and are indispensable either for the development of embryonic hematopoiesis or for the expansion of HSCs, but their precise roles in maintenance of adult HSCs were largely unknown. However, of particular note is a recent report that SCL, a transcription factor, indispensable for the development of primitive erythropoiesis at the embryonic stage, is not essential for the maintenance of adult hematopoietic, although it is still required for erythroid and megakaryocytic differentiation of the committed progenitor cells.[11] In addition, Kunisato et al[12] demonstrated that SCL does not affect long term repopulating capacity of HSCs but direct their commitment to myeloid lineage using retrovirus-mediated gene transfer of a dominant-negative SCL mutant into HSCs. These findings on *SCL*-null mice are comparable to those on our *Runx1*-null animals, where Runx1 is required specifically for embryonic development of definitive hematopoiesis and regulation of lymphoid differentiation and megakaryocytic maturation, but is also dispensable for the maintenance of adult HSCs. Both examples may represent the functional multi-modality of hematopoietic transcription factors that participated in exquisite regulation of development and maintenance of hematopoietic systems. In our *Runx1*-null mice, there was the increased number of hematopoietic progenitor cells as well as the augmented replating capacity of these progenitors from the *Runx1*-knockout bone marrow. Because *Runx1* is mutated in FPD/AML[13] as well as some sporadic MDS cases,[14-16] it is intriguing in view of the leukemogenic role of Runx1 deficiency that the expansion of hematopoietic progenitors and increased self-renewal capacity have also been observed in the mouse models of t(8;21) (q21;q22)-carrying leukemias, indicating that the size of progenitor cell pool seems to be negatively regulated by Runx1 function, which may be overridden by AML-1-ETO. Although it is not clear whether the increased progenitor pool reflects differentiation block of downstream cell lineages or unregulated cell cycling or apoptosis of the progenitors, it may well be possible that the expanded progenitor pool also

contribute to leukemia development by, for example, increasing the chance of additional mutations. It should also be noted that neither *Runx1*-null mice nor murine models of t(8;21)(q21;q22) develop spontaneous leukemia, indicating additional mutations are required for development of full-blown leukemia.

As already mentioned, the *Runx1*-null mice show greatly reduced platelet counts with severely impaired maturation of megakaryocytes as evident from their smaller cell size, hypoploidy, and abnormalities in ultrastructure. Although the precise mechanism of this phenotype is still unclear, it is worth noting that the similar megakaryocytic maturation arrest at the polyploidization step is also observed in *Fli-1* knockout mice and *GATA-1* knockdown mice.[17-19] Since Runx1 and GATA-1 are known to physically interact with each other in megakaryocytes and promote megakaryocyte-specific gene expression,[20] it may be speculated that Runx1 regulates megakaryocytic maturation in cooperation with GATA-1 through affecting megakaryocyte-specific gene expression.

Mature lymphocyte production is also severely defective in both T and B lineages and competitively transplanted *Runx1*-null HSCs could not contribute to recipients' T or B populations in spite of the normal number of common lymphoid progenitors. *Runx1* is expressed in the developing thymocytes and in B cells, and is known to regulate the expression of T cell and B cell-specific genes. A previous study using T-cell specific *Runx1* knockout mice revealed the essential role of Runx1 in T cell development, in which Runx1 was shown to be required for development of double negative ($CD4^-CD8^-$) thymocytes in transition from $CD44^-CD25^+$ (DN3) to $CD44^-CD25^-$ (DN4) phenotypes.[21] However, our bone marrow reconstitution experiment using Runx1-null hematopoietic stem cells also demonstrated that Runx1 expression is absolutely required for more early stages of T cell development in transition from $CD44^+CD25^+$ (DN2) to DN3 double negative thymocytes. On the other hand, no direct evidence has been reported about the exact biological role of Runx1 in B cell development. Runx1-null bone marrow cells could not repopulate the peripheral T and B lymphocyte population of sublethally irradiated recipients while CLP fraction of the conditional knockout animals is not decreased. Therefore, our data revealed the previously unknown role of Runx1 in B cell development. The precise regulation of Runx1 in B cell development should be analyzed by further investigation, and B-cell lineage-specific targeting of the Runx1 gene is under way to clarify the physiological role of Runx1 in the committed B cells.

In conclusion, from the analysis of conditional Runx1-knockout mice, it became clear that Runx1 is not required for the maintenance of HSC functions in adult mice, but is indispensable for maturation and differentiation of various blood components including T and B lymphocytes, as well as megakaryocytes (Fig. 1). Our data not only recapitulate the human diseases FPD/AML and MDS related to Runx1, but also demonstrate that Runx1 is still a multi-role regulator in maintenance of the lineage-committed cells in adult hematopoiesis, although for HSCs, it is essential only once at the embryonic developmental stage.

References

1. Dzierzak E, Medvinsky A. Mouse embryonic hematopoiesis. Trend Genet 1995; 11:359-66.
2. Medvinsky A, Dzierzak E. Definitive hematopoiesis is autonomously initiated by the AGM region. Cell 1996; 86:897-906.
3. Lutterbach B, Hiebert SW. Role of the transcription factor AML-1 in acute leukemia and hematopoietic differentiation. Gene 2000; 245:223-35.
4. Okuda T, van Deursen J, Hiebert SW, Grosveld G, Downing JR. AML1, the target of multiple chromosomal translocations in human leukemia, is essential for normal fetal liver hematopoiesis. Cell 1996; 84:321-30.
5. Wang Q, Stacy T, Binder M, Marin-Padilla M, Sharpe AH, Speck NA. Disruption of the *Cbfa2* gene causes necrosis and hemorrhaging in the central nervous system and blocks definitive hematopoiesis. Proc Natl Acad Sci USA 1996; 93:3444-9.
6. North TE, de Bruijn MF, Stacy T, Talebian L, Lind E, Robin C, et al. Runx1 expression marks long-term repopulating hematopoietic stem cells in the midgestation mouse embryo. Immunity 2002; 16:661-72.
7. Rhoades KL, Hetherington CJ, Harakawa N, Yergeau DA, Zhou L, Liu LQ, et al. Analysis of the role of AML1-ETO in leukemogenesis, using an inducible transgenic mouse model. Blood 2000; 96:2108-15.
8. de Guzman CG, Warren AJ, Zhang Z, Gartland L, Erickson P, Drabkin H, et al. Hematopoietic stem cell expansion and distinct myeloid developmental abnormalities in a murine model of the AML1-ETO translocation. Mol Cell Biol 2002; 22:5506-17.
9. Higuchi M, O'Brien D, Kumaravelu P, Lenny N, Yeoh EJ ,Downing JR. Expression of a conditional AML1-ETO oncogene bypasses embryonic lethality and establishes a murine model of human t(8;21) acute myeloid leukemia. Cancer Cell 2002; 1:63-74.
10. Ichikawa M, Asai T, Saito T, Yamamoto G, Seo S, Yamazaki I, et al. AML-1 is required for megakaryocytic maturation and lymphocytic differentiation, but not for maintenance of hematopoietic stem cells in adult hematopoiesis. Nat Med 2004; 10:299-304.
11. Mikkola HK, Klintman J, Yang H, Hock H, Schlaeger TM, Fujiwara Y, et al. Haematopoietic stem cells retain long-term repopulating activity and multipotency in the absence of stem-cell leukaemia SCL/tal-1 gene. Nature 2003; 421:547-51.
12. Kunisato A, Chiba S, Saito T, Kumano K, Nakagami-Yamaguchi E, Yamaguchi T, et al. Stem cell leukemia (SCL) directs hematopoietic stem cell fate. Blood 2004; 103:3336-41.
13. Song WJ, Sullivan MG, Legare RD, Hutchings S, Tan X, Kufrin D, et al. Haploinsufficiency of CBFA2 causes familial thrombocytopenia with propensity to develop acute myelogenous leukaemia. Nat Genet 1999; 23:166-75.
14. Osato M, Asou N, Abdalla E, Hoshino K, Yamasaki H, Okubo T, et al. Biallelic and heterozygous point mutations in the runt domain of the AML1/PEBP2alphaB gene associated with myeloblastic leukemias. Blood 1999; 93:1817-24.
15. Imai Y, Kurokawa M, Izutsu K, Hangaishi A, Takeuchi K, Maki K, et al. Mutations of the AML1 gene in myelodysplastic syndrome and their functional implications in leukemogenesis. Blood 2000; 96:3154-60.
16. Preudhomme C, Warot-Loze D, Roumier C, Grardel-Duflos N, Garand R, Lai JL, et al. High incidence of biallelic point mutations in the Runt domain of the AML1/PEBP2 alpha B gene in Mo acute myeloid leukemia and in myeloid malignancies with acquired trisomy 21. Blood 2000; 96:2862-9.
17. Shivdasani RA, Fujiwara Y, McDevitt MA, Orkin SH. A lineage-selective knockout establishes the critical role of transcription factor GATA-1 in megakaryocyte growth and platelet development. EMBO J 1997; 16:3965-73.
18. Takahashi S, Komeno T, Suwabe N, Yoh K, Nakajima O, Nishimura S, et al. Role of GATA-1 in proliferation and differentiation of definitive erythroid and megakaryocytic cells in vivo. Blood 1998; 92:434-42.
19. Hart A, Melet F, Grossfeld P, Chien K, Jones C, Tunnacliffe A, et al. Fli-1 is required for murine vascular and megakaryocytic development and is hemizygously deleted in patients with thrombocytopenia. Immunity 2000; 13:167-77.
20. Elagib KE, Racke FK, Mogass M, Khetawat R, Delehanty LL, Goldfarb AN. RUNX1 and GATA-1 coexpression and cooperation in megakaryocytic differentiation. Blood 2003; 101:4333-41.
21. Taniuchi I, Osato M, Egawa T, Sunshine MJ, Bae SC, Komori T, et al. Differential requirements for Runx proteins in CD4 repression and epigenetic silencing during T lymphocyte development. Cell 2002; 111:621-33.

JOURNAL OF CLINICAL MICROBIOLOGY, June 2004, p. 2733–2741 Vol. 42, No. 6
0095-1137/04/$08.00+0 DOI: 10;1128/JCM.42.6.2733–2741.2004

Prospective Comparison of the Diagnostic Potential of Real-Time PCR, Double-Sandwich Enzyme-Linked Immunosorbent Assay for Galactomannan, and a (1→3)-β-D-Glucan Test in Weekly Screening for Invasive Aspergillosis in Patients with Hematological Disorders

Masahito Kawazu,[1] Yoshinobu Kanda,[1,2] Yasuhito Nannya,[1] Katsunori Aoki,[1] Mineo Kurokawa,[1] Shigeru Chiba,[1,2] Toru Motokura,[1] Hisamaru Hirai,[1,2] and Seishi Ogawa[1,3]*

Department of Hematology and Oncology,[1] Department of Cell Therapy and Transplantation Medicine,[2] and Department of Regeneration Medicine for Hematopoiesis,[3] Graduate School of Medicine, University of Tokyo, Tokyo 113-8655, Japan

Received 30 October 2003/Returned for modification 11 December 2003/Accepted 18 February 2004

The establishment of an optimal noninvasive method for diagnosing invasive aspergillosis (IA) is needed to improve the management of this life-threatening infection in patients with hematological disorders, and a number of noninvasive tests for IA that target different fungal components, including galactomannan, (1→3)-β-D-glucan (BDG), and *Aspergillus* DNA, have been developed. In this study, we prospectively evaluated the diagnostic potential of three noninvasive tests for IA that were used in a weekly screening strategy: the double-sandwich enzyme-linked immunosorbent assay (ELISA) for galactomannan (Platelia Aspergillus), a real-time PCR assay for *Aspergillus* DNA (GeniQ-Asper), and an assay for BDG (β-glucan Wako). We analyzed 149 consecutive treatment episodes in 96 patients with hematological disorders who were at high risk for IA and diagnosed 9 proven IA cases, 2 probable IA cases, and 13 possible invasive fugal infections. In a receiver-operating characteristic (ROC) analysis, the area under the ROC curve was greatest for ELISA, using two consecutive positive results (0.97; $P = 0.036$ for ELISA versus PCR, $P = 0.055$ for ELISA versus BDG). Based on the ROC curve, the cutoff for the ELISA could be reduced to an optical density index (O.D.I.) of 0.6. With the use of this cutoff for ELISA and cutoffs for PCR and BDG that give a comparable level of specificity, the sensitivity/specificity/positive predictive value/negative predictive value of the ELISA and the PCR and BDG tests were 1.00/0.93/0.55/1.00, 0.55/0.93/0.40/0.96, and 0.55/0.93/0.40/0.96, respectively. In conclusion, among these weekly screening tests for IA, the double-sandwich ELISA test was the most sensitive at predicting the diagnosis of IA in high-risk patients with hematological disorders, using a reduced cutoff of 0.6 O.D.I.

Invasive aspergillosis (IA) is one of the most serious complications in patients with hematological malignancies. It has an extremely high mortality rate (11) and affects not only terminally ill patients with refractory leukemia or lymphoma but also patients who could otherwise be expected to experience a potential cure of the underlying leukemia or lymphoma. Among several factors that contribute to the high mortality rate, difficulties in establishing a reliable diagnosis early enough for successful intervention have been repeatedly discussed (10). A definitive diagnosis usually requires invasive tissue sampling, which is often hampered by the critical condition of the patients, while a delay in initiating antifungal therapy, or, conversely, a hasty use of empiric or prophylactic amphotericin B before making a definitive diagnosis may result in treatment failure for full-blown infection or excess toxicity, respectively.

To overcome this problem and to improve the treatment outcome, advances have been made over the past decade in the fields of both diagnostics and therapeutics, including improvements in diagnostic imaging (7, 8, 18) and histopathology (1), and the development of broad-spectrum antifungal agents with low toxicities (4, 24, 29, 33). In the field of diagnostics, much attention has recently been given to the development of several types of noninvasive laboratory tests for IA. These tests are designed to sensitively detect circulating *Aspergillus* components and include a double-sandwich enzyme-linked immunosorbent assay (ELISA) for galactomannan (GM) antigen (Platellia Aspergillus) (30), tests for (1→3)-β-D-glucan (BDG) (β-glucan Wako or FungiTec G test) (23, 25), and a number of PCR-based assay systems for *Aspergillus* DNA (5, 6, 12, 34).

The ELISA for GM uses a rat monoclonal antibody directed against the 1→5-β-galactofuranoside side chains of the GM molecule as both the capture and detection antibodies for ELISA and can detect as little as 1.0 ng of circulating GM per ml (30). The excellent sensitivity and specificity of this assay have been repeatedly demonstrated and validated in tests of patients with hematological disorders (22, 27, 32). BDG is a ubiquitous component of diverse fungal species and a possible target for the diagnostic detection of IA. Two assay systems are currently available for the sensitive detection of circulating

* Corresponding author. Mailing address: Department of Regeneration Medicine for Hematopoiesis, Graduate School of Medicine, University of Tokyo, 7-3-1 Hongo, Bunkyo-ku, Tokyo 113-8655, Japan. Phone: 81-3-5800-6421. Fax: 81-3-5804-6261. E-mail: sogawa-tky@umin.ac.jp.

BDG, and both are based on the *Limulus* reaction, in which a trace amount of BDG can trigger a horseshoe crab coagulation cascade through factor G (23, 25). The BDG test is a useful method for screening for invasive fungal infection (IFI) and is widely used in Japan. The other test that has long been under intensive investigation for the sensitive detection of IA is PCR amplification of *Aspergillus* DNA, mainly of the 18S ribosomal gene (5, 6, 12, 34). Moreover, recently introduced real-time PCR designs have made it possible to quantitatively evaluate a fungal load with high sensitivity (9, 17, 21).

With regard to an antifungal strategy, it would be interesting to determine which of these tests is the best for diagnosing IA in patients with hematological disorders. Although high sensitivity and specificity are reported for PCR-based assays, the question whether PCR-based assays are superior to GM ELISA is still controversial (3, 5, 19, 34). Previously, we developed a sensitive real-time PCR system for detecting *Aspergillus* 18S ribosomal DNA, with which as few as 40 copies of aspergillus DNA per ml of plasma could be stably detected. We reported that the sensitivity of our real-time PCR for IA in 33 IA patients was higher than those of the double-sandwich ELISA for GM and the BDG test, with only a slightly lower specificity than that of GM ELISA (17). However, this previous study may have been biased by its partially retrospective design, limited sampling points in each case or infectious episode, and use of an inappropriately high cutoff value for ELISA. In the present purely prospective analysis, we consecutively enrolled 96 patients with hematological disorders who were at high risk for IA, monitored the levels of *Aspergillus* DNA, GM, and BDG in plasma, as well as the development of IA, at weekly intervals, and evaluated their diagnostic potentials by using receiver-operating characteristic (ROC) analyses.

MATERIALS AND METHODS

Study population and design. From March 2001 through April 2002, a consecutive series of adult patients with hematological disorders who had been admitted to our hospital and were thought to be at high risk for IA were enrolled in the study, and their levels of *Aspergillus* DNA in plasma and GM in serum, and BDG in plasma were monitored weekly. Patients were considered to be at high risk for IA if (i) they underwent chemotherapy and were expected to be neutropenic (less than 500 neutrophils per μl) for at least 10 days, (ii) they had refractory disease or were neutropenic and presented for more than 96 h with persistent fever that was refractory to appropriate broad-spectrum antibacterial treatments, (iii) they had presented with acute graft-versus-host disease (GVHD) of grade 2 or greater or had extensive chronic GVHD, or (iv) they had received corticosteroids for more than 3 weeks within the previous 60 days. Plasma *Aspergillus* DNA levels, serum GM levels, and plasma BDG levels were to be measured once weekly whenever the patients were thought to be at high risk. Each period during which measurement was performed was defined as one treatment episode. Omission of sampling was permitted unless two consecutive samples were lacking. Treatment episodes with only one or two samples for each test were excluded from the analysis.

The level of *Aspergillus* DNA in plasma was measured using real-time PCR, as described previously (17). The ELISA for GM (Platelia Aspergillus; Sanofi Diagnostics Pasteur, Marnes-La-Cosuette, France) and the β-glucan Wako test (Wako Pure Chemical Industries, Ltd., Tokyo, Japan) were performed as specified by the manufacturers. Each sample was tested twice for GM and BDG, and the average of the two measurements was taken.

Antifungal prophylaxis consisted of daily administration of 200 mg of fluconazole or itraconazole capsules with or without 15 mg of aerosolized amphotericin B or 10 mg of intravenous amphotericin B for patients with a suspected history of IA. Neutropenic fever was treated with broad-spectrum antibiotics in accordance with the published guidelines (16). Blood samples were used for bacterial, mycobacterial, and fungal cultures prior to the initiation of antibiotics. When IFI was suspected, treatment with 1 mg intravenous amphotericin B per kg was initiated. During the febrile period, patients were intensively surveyed for possible sites of infection and causative microorganisms. Diagnostic procedures included routine cultures of urine and stools, repeated cultures of blood and sputum, weekly chest X rays, high-resolution computed tomography (CT) scan of the chest, and, when possible, bronchoscopic examinations and open biopsies.

Case definitions. For each treatment episode, a diagnosis was made following the published case definition criteria for invasive fungal infections from the European Organization for Research and Treatment of Cancer/Invasive Fungal Infections Cooperative Group and the National Institute of Allergy and Infectious Diseases Mycoses Study Group (EORTC-IFICG and NIAID-MSG) (2), with the necessary modification that the plasma GM level was not included in the microbiological criteria.

Statistical analysis. As described by Maertens et al. (22), we made a set of different estimates (A/B, C, and D) for the sensitivity, specificity, positive predictive value (PPV), and negative predictive value (NPV) of each test, where different definitions of disease status for an episode were used to calculate these statistical indexes, since there is an intrinsic uncertainty regarding the true disease status of IA so that the calculation of these values could be significantly affected by the definition of the disease status. Estimate A/B defines "proven IA" and "probable IA" as truly positive and only "no IA" as truly negative, whereas estimates C and D incorporate "possible IFI" into the truly positive and truly negative groups, respectively. In all of the estimates, "no-IA" episodes were considered truly negative. Since our objective was to validate and compare the potentials of different diagnostic tests in a setting where these tests are performed weekly to monitor the development of IA, the positivity or negativity of a test was defined for each episode, where an episode was considered positive if at least one sample (method I), or any two consecutive samples (method II) became positive. There is also a practical reason for this approach. The onset and resolution of an IA episode are not always clear and, indeed, are rather poorly defined in many cases. Even in proven cases, there might be several febrile episodes and the onset might be insidious. In this setting, the sample-based calculation of sensitivity and specificity might be severely biased. In addition, we determined a proper cutoff value for each test through a ROC analysis, in which sensitivity and specificity were calculated as a function of the cutoff value, (1 − specificity) was plotted against the sensitivity, and the areas under the ROC curves (AUCs) were calculated. The significance of the difference in the AUCs of any two diagnostic measures was statistically tested as described above, and *P* values were calculated by the paired method under the null hypothesis that the two ROC curves represent random samples from similar underlying data for sensitivities and specificities (13). Therefore, the *P* values can be used only to compare two ROC curves at a time. The calculated *P* values reflect the one-tailed significance of difference between two ROC curves.

RESULTS

Study episodes. There were 149 treatment episodes in 96 consecutive patients, including 9 proven IA, 2 probable IA, 13 possible IFI, and 125 no-IA episodes. Of these, 56 episodes (38%) were associated with stem cell transplantation. The patient characteristics and sample distributions are summarized in Table 1. Nineteen treatment episodes had no host factors. Overall, 1,251 samples were analyzed by the real-time PCR assay, 1,233 were analyzed by double-sandwich ELISA for GM, and 1,243 were analyzed by the BDG test. On average, approximately eight samples were examined for each treatment episode. The characteristics of the 24 episodes of proven IA, probable IA, and possible IFI are shown in Table 2. There were 24 fatal episodes, of which 8 were proven IA, 1 was probable IA, 4 were possible IFI, and 11 were no IA. Autopsies were performed in 14 episodes (58%), including 6 proven IA and 8 no-IA cases. In the remaining 10 fatal episodes, autopsy was not permitted by the patients' families. The 3 proven IA episodes were diagnosed based on histopathology of a pharyngeal biopsy specimen, a surgical specimen of the brain, and a skin biopsy specimen, respectively. Although postmortem examinations disclosed superinfections of disseminated *Trichosporon* infection and atypical mycobacteriosis in episode 1 and

TABLE 1. Patient characteristics

Characteristic	Patients with:				Total[b]
	Proven IA	Probable IA	Possible IFI	No IA	
No. of episodes	9	2	13	125	149 (96)
No. of deaths	8	1	4	11	24
No. of autopsies	6	0	0	8	14
Age (yr)					
Mean	46	47	43	45	45
Median	42	47	40	47	46
Range	19–69	40–53	18–68	17–74	17–74
Sex (no. male/no. female)	6/3	2/0	12/1	82/43	102/47 (67/29)
No. with disease[a]					
AML	3	1	5	48	57 (29)
ALL	1	0	4	26	31 (19)
CML	0	1	2	8	11 (9)
MDS	3	0	2	11	16 (14)
NHL	2	0	0	28	30 (21)
AA	0	0	0	2	2 (2)
Other	0	0	0	2	2 (2)
No. with allografts	4	2	6	44	56
Duration of episode (days)					
Mean	126	92	78	50	57
Median	135	92	57	37	43
Range	36–234	50–134	35–172	11–181	11–234
No. with host factor:					
Neutropenia	7	1	8	86	102
Fever	6	1	7	37	51
GVHD	2	2	5	17	26
Steroid	2	1	4	28	35
None	1	0	0	18	19
Duration of neutropenia (days)					
Mean	63	10	42	16	21
Median	37	10	18	14	15
Range	0–205	0–20	0–162	0–120	0–205
No. of samples tested					
PCR	154	25	146	926	1,251
Mean (per episode)	17.1	12.5	11.2	7.4	8.4
Median (per episode)	17	13	9	6	6
Range (per episode)	7–32	6–19	4–24	3–26	3–32
GM	155	24	140	914	1,233
Mean (per episode)	17.2	12.0	10.8	7.3	8.3
Median (per episode)	18	12	9	5	6
Range (per episode)	7–30	5–19	5–24	2–26	2–30
BDG	158	24	147	914	1,243
Mean (per episode)	17.6	12.0	11.3	7.3	8.3
Median (per episode)	19	12	9	6	6
Range (per episode)	7–31	5–19	6–24	3–23	3–31

[a] AML, acute myelogenous leukemia; ALL, acute lymphocytic leukemia; CLL, chronic nyelogenous leukemia; MDS, myelodysplastic syndrome; NHL, non-Hodgkin lymphoma; AA, aplastic anemia.
[b] Values in parentheses are numbers of patients. Other values refer to numbers of episodes.

episode 9, respectively, no invasive candidiasis was documented during the study period.

Among the 125 no-IA episodes, 11 deaths occurred, and the diagnosis of no IA was confirmed by autopsy in 8. The other three fatal episodes were not confirmed by autopsy and included two respiratory failures following chemotherapy and one case of severe stomatitis following a second bone marrow transplantation. One respiratory failure was due to bacterial pneumonia, in which *Pseudomonas aeruginosa* was cultured from the sputum and the blood. In the other episode, respiratory failure developed in association with rapid tumor growth. Although no pathogen was identified despite repeated cultures, we could not completely exclude a possible infectious origin of this episode. The episode of severe stomatitis became suddenly fatal after the patient aspirated the clot and was asphyxiated.

ROC analysis. Figure 1 shows ROC curves for each test, using different definitions of the disease status. First, we examined the behaviors of the ROC curves for different diagnostic tests by using an "ideal" estimate (estimate A/B), in which episodes were expected to be most accurately defined. ELISA has a larger AUC in both method I (ELISA, 0.93; PCR, 0.81; BDG, 0.85) and method II (ELISA, 0.97; PCR, 0.76; BDG, 0.79). To increase the sensitivity for GM, we could more easily decrease its cutoff value with a small decrease in specificity. In contrast, a higher sensitivity could be obtained for the PCR and BDG tests by decreasing their cutoff values, but this would be at a significant cost in terms of specificity. When we shifted the diagnostic algorithm from method I (one positive sample) to method II (two consecutive positive samples), the AUC for the GM test was further increased while those for the PCR and BDG tests decreased, indicating that the GM test has higher

TABLE 2. Diagnosis of IA and its documentation

Episode no.	Patient characteristics[a]: Age (yr)	Sex	IA	Primary disease	Status of primary disease	Outcome	Host factors	Clinical evidence	Culture and its source	Histological evidence	Maximum value (method I/method II): PCR (copies/ml)	GM (O.D.I.)	BDG (ng/ml)
1	41	F	P	AML M1	Post-allo, RD	Dead	NF	Erosion of sinus walls	*A. flavus* and *A. fumigatus* from pharyngeal mucosa	Biopsy	2,000/200	3.8/3.6	19.7/4.7
2	32	M	P	MDS (RAEB-t)	Post-allo, CR	Dead	GS	Dyspnea, pleural effusion		Autopsy	32/0	1.3/1.0	60.5/36.5
3	58	M	P	AML M1	RD	Dead	NF	Halo sign		Autopsy	90/42.5	7.7/6.4	25/1.5
4	38	F	P	AML M2	Post-allo, CR	Alive	NS	Cavity within area of consolidation	*A. fumigatus* from broncheal lavage fluid	Biopsy	33.5/0	1.9/1.7	2.8/0
5	51	M	P	Macroglobulinemia	Stable disease	Dead	None	Extensive skull base destruction	*A. fumigatus* from epidural abscess	Biopsy	0/0	1.2/0.8	37.4/7.1
6	19	M	P	MDS RA	RD	Dead	NF	Multiple nodular lesions in the lung field, pleural effusion		Autopsy	3,500/1,000	2.5/1.5	155.5/59.2
7	42	M	P	MDS/AML	Post-allo, RD	Dead	NFG	Dyspnea, pleural effusion		Autopsy	24/9	2.4/0.6	0/0
8	63	F	P	ATL acute type	RD	Dead	NF	Dyspnea, pleural effusion		Autopsy	50/12.5	1.9/0.7	2.4/0
9	69	M	P	ALL PreB	RD	Dead	NF	No specific clinical evidence		Autopsy	100,000/5,000	4.2/1.1	171.7/12.6
10	53	M	PP	AML M2	Post-allo, CR	Dead	FG	Dyspnea, pleural effusion	*A. spergillus* spp. from bronchoalveolar lavage fluid	NA[b]	5/0	5.3/0.7	4.5/2.2
11	40	M	PP	CML CP1	Post-allo, CR	Alive	NGS	Halo sign	*A. fumigatus* from sputum	NA	11.5/7.5	2.3/2.0	0/0
12	68	M	PPP	MDS/AML	RD	Dead	NF	Multiple nodular lesions in the lung field, intraparenchymal brain mass lesion, seizure, hemiparesis		NA	155/100	2.2/1.5	18.3/16.6
13	24	M	PPP	AML M4E	CR, HDAraC	Alive	NF	Nodular skin lesion without any other explanation, multiple nodular lesions in the lung field		NA	20.5/0	4.5/0.3	0/0
14	61	M	PPP	AML M4E	CR, HDAraC	Alive	N	Halo sign		NA	1,000/9	0.2/0.1	3.5/2.9
15	30	M	PPP	ALL precursor B	Post-allo, CR	Alive	NFGS	Nonspecific abnormal shadow in lung field, pleural effusion		NA	60/60	0.6/0.4	0/0
16	61	M	PPP	AML M2	RD	Dead	NF	Multiple nodular lesions in the lung field, halo sign, cavity within area of consolidation		NA	84.5/0	1.1/0.7	2/0
17	68	M	PPP	CML BC	RD	Dead	NS	Dyspnea, pleural effusion		NA	165/0	0.3/0.2	0/0
18	25	M	PPP	ALL precursor B	RD	Alive	NG	Cavity within area of consolidation		NA	400/0	0.7/0.6	3.2/0
19	32	M	PPP	ALL PreB	Post-allo, CR	Dead	FGS	Dyspnea, pleural effusion		NA	27/1	0.7/0.5	3.7/2.4
20	18	F	PPP	AML M2	CR, HDAraC	Alive	N	Halo sign		NA	0/0	0.6/0.1	0/0
21	55	M	PPP	MDS RA	Stable disease	Alive	F	Cough, dyspnea, pleural effusion		NA	19/4	0.8/0.3	0/0
22	28	M	PPP	CML CP1	Post-allo, CR	Alive	G	Cough, dyspnea, pleural effusion		NA	0/0	0.4/0.3	0/0
23	40	M	PPP	CML CP1	Post-allo, CR	Alive	GS	Cough, dyspnea, new infiltrate not fulfilling the major radiological criteria without an alternative diagnosis		NA	6/0	0.5/0.4	0/0
24	54	M	PPP	ALL precursor B	Post-allo, CR	Alive	F	Dyspnea, new infiltrate not fulfilling the major radiological criteria without an alternative diagnosis		NA	10.5/0	0.5/0.3	0/0

[a] F, female; M, male; P, proven; PP, probable; PPP, possible; AML, acute myeloid leukemia; MDS, myelodysplastic syndrome; RA, refractory anemia; RAEB-t, RA with excess of blasts in transformation; ALL, acute lymphoblastic leukemia/lymphoma; CML, chronic myelogenous leukemia; CP, chronic phase; BC, blastic crisis; allo, allogencic hematopoietic stem cell transplantation; CR, complete remission; RD, refractory disease; HDAraC, high-dose cytrabine; N, neutropenia; F, persistent fever; G, GVHD, S, prolonged use of corticosteroid.

[b] NA, not available.

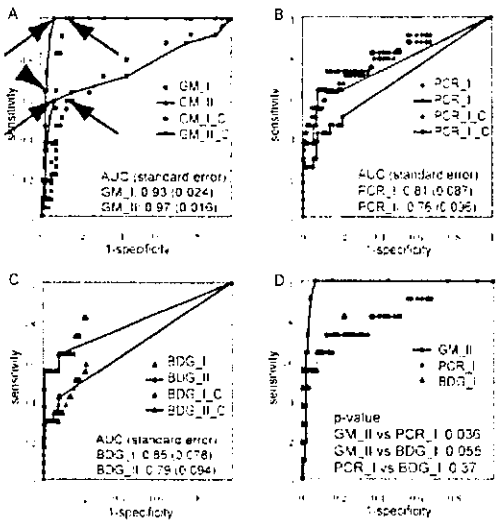

FIG. 1. (A to C) ROC curves of the GM (A), PCR (B), and BDG (C) tests for screening for IA. Both methods I and II were used. The ROC curves obtained by estimate A/B are shown in red, and those obtained by estimate C are shown in blue. The ROC curves obtained by method II are indicated by solid lines, and those obtained by method I are indicated by dotted lines. (D) Combination of ROC curves of the GM test (method II) and those of the PCR and BDG tests (method I).

reproducibility than the other two tests. The comparison of ROC curves of ELISA (method II), PCR (method I), and BDG (method I) is presented in Fig. 1D. When estimate C was applied for ROC analyses, these characteristics of the ROC curve for GM were partially obscured. In estimate C, a large decrease in sensitivity shifted the ROC curve downward and caused a significant reduction in AUC for the ELISA and BDG test, as expected. On the other hand, the ROC curve for the PCR test did not significantly change, since an expected decrease in sensitivity due to false-positive episodes in the possible IFI group is thought to be counterbalanced by a gain due to false-positive PCR results in these episodes. The ROC curves for the GM test in estimates A/B, C, and D, which is not presented but is similar to that for A/B, represent extreme cases, and the unknown "real" ROC curve might be mapped between these extremes.

Optimal cutoff value. Determination of an optimal cutoff value may be somewhat arbitrary depending on the purpose of the diagnostic test. A loss of specificity may be allowed to obtain a higher sensitivity. Based on the conventional or manufacturer-recommended cutoff values, an optical density index (O.D.I.) of 1.0, in two serial samples for GM (2, 22), i.e., 40 copies/ml for PCR and 11 pg/ml for the BDG test, all tests showed excellent specificity (0.98) in estimate A/B whereas their sensitivity was generally low (0.64, for GM, 0.45 for the PCR test, and 0.55 for the BDG test) even in estimate A/B, with further decreases as low as 0.33 for the GM test and 0.29 for the BDG test in estimate C. The current standard for ELISA (red arrowhead in Fig. 1A) seems to be inadequate. It could be reduced to 0.6 O.D.I. in method II (red arrows in Fig. 1A), or the criteria for positivity could be relaxed to those in method I while retaining the same cutoff (1.0 O.D.I.) (blue arrows), without great loss of specificity. With regard to specificity, the former may be recommended ($P = 0.0334$ by Fisher's direct test), which reflects a more leftward displacement of the ROC curve for method II. Both cutoff values represent the inflexion point of each ROC curve, around which the diagnostic efficacy is maximum for both cutoffs. The sensitivity/specificity and PPV/NPV of the GM test are 1.0/0.93 and 0.55/1.0 for a cutoff value of 0.6 O.D.I. in method II and 1.0/0.86 and 0.38/1.0 for a cutoff value of 1.0 O.D.I. in method I. Various diagnostic statistical parameters in different calculations are presented in Table 3. We may improve the diagnostic efficiency by using two or three tests in combination. In our analyses, however, we could not obtain better sensitivity by combination use of multiple tests employing much reduced cutoff values while maintaining high specificity (data not shown). This is also accompanied by significant delay of diagnosis.

Time interval between the first positive result and the antemortem diagnosis. Chronological relationships between the first positive results of different screening tests, histopathology, and diagnostic imaging are summarized in Fig. 2 and 3. For the PCR and BDG tests, the conventional cutoff was used, while the second of the first two consecutive results equal to or greater than 0.6 or 1.0 O.D.I. was plotted for ELISA. When the new reduced cutoff was used, the first positive date for GM was brought forward by a median of 10 (0 to 70, $n = 9$, mean = 24) days compared to the conventional cutoff value. Using the conventional cutoff, only one episode was identified to have a positive ELISA result before definitive treatment was started. In contrast, with the new reduced cutoff, the first positive ELISA result preceded the initiation of broad-spectrum antifungal treatment in seven IA-positive episodes (median, 31 days; range, 2 to 127 days; mean, 28 days). It became positive 51 days before a positive histopathology result (10 to 127 days; mean, 31 days).

Unfortunately, chronological comparisons between the three different assays were possible for only six episodes, in which patients had refractory leukemia and their IA tended to have a rapidly progressive course as a terminal infection (Fig. 3). In these episodes, ELISA gave positive findings earlier than (five episodes) or at the same time as (one episode) the BDG test (median, 16.5 days; range, 0 to 76 days). The PCR test was positive in 11 of 24 IA patients in estimate C. A comparison was possible in 5 of the 11 episodes, which were also positive for ELISA, but there was no significant difference in the date of the first positive result between ELISA and the PCR tests.

DISCUSSION

In this study, we compared the diagnostic potential of three different laboratory tests used to screen for IA in a prospective setting, where GM, DNA, and BDG levels in a cohort of patients at high risk for IA were measured weekly. The statistical parameters of a diagnostic test can be dramatically affected by the predetermined cutoff value, and when there is some uncertainty regarding the disease status, as in this case, they can also be influenced by the definition of the disease status. Therefore, to meaningfully compare the diagnostic potentials of these different tests, we performed an ROC analysis for each test by using the same cohort of patients with different positive result criteria (methods I and II) and various definitions of the disease status (estimates A/B, C, and D). As a

TABLE 3. Statistics for some selected thresholds

Method and threshold	Sensitivity A/B (C)	Specificity A/B (D)	PPV A/B (D)	NDV A/B (C)	Efficacy A/B (C)
Method I					
GM (O.D.I.)					
0.5	1.00 (0.88)	0.34 (0.33)	0.12 (0.11)	1.00 (0.93)	0.40 (0.43)
0.6	1.00 (0.79)	0.55 (0.54)	0.16 (0.15)	1.00 (0.93)	0.59 (0.59)
1.0	1.00 (0.58)	0.86 (0.85)	0.38 (0.34)	1.00 (0.91)	0.87 (0.81)
1.5	0.82 (0.46)	0.90 (0.89)	0.41 (0.38)	0.98 (0.90)	0.89 (0.83)
PCR (copies/ml)					
5	0.91 (0.88)	0.43 (0.41)	0.12 (0.11)	0.98 (0.95)	0.47 (0.30)
10	0.82 (0.79)	0.60 (0.55)	0.15 (0.13)	0.97 (0.94)	0.62 (0.63)
20	0.73 (0.67)	0.78 (0.75)	0.23 (0.19)	0.97 (0.92)	0.78 (0.77)
40	0.45 (0.46)	0.98 (0.93)	0.63 (0.36)	0.95 (0.90)	0.93 (0.89)
BDG (ng/ml)					
2	0.82 (0.58)	0.77 (0.76)	0.24 (0.21)	0.98 (0.91)	0.78 (0.74)
3	0.64 (0.46)	0.84 (0.82)	0.26 (0.23)	0.96 (0.89)	0.82 (0.78)
5	0.55 (0.29)	0.92 (0.92)	0.38 (0.35)	0.96 (0.87)	0.89 (0.82)
11	0.55 (0.29)	0.98 (0.97)	0.67 (0.60)	0.96 (0.88)	0.94 (0.87)
Method II					
GM (O.D.I.)					
0.5	1.00 (0.63)	0.84 (0.83)	0.35 (0.31)	1.00 (0.92)	0.85 (0.81)
0.6	1.00 (0.58)	0.93 (0.91)	0.55 (0.48)	1.00 (0.92)	0.93 (0.87)
1.0	0.64 (0.33)	0.98 (0.97)	0.70 (0.64)	0.97 (0.88)	0.95 (0.87)
1.5	0.45 (0.25)	0.98 (0.97)	0.63 (0.56)	0.95 (0.87)	0.93 (0.86)
PCR (copies/ml)					
5	0.64 (0.43)	0.87 (0.86)	0.30 (0.27)	0.96 (0.89)	0.85 (0.80)
10	0.45 (0.30)	0.94 (0.93)	0.38 (0.33)	0.95 (0.88)	0.90 (0.84)
20	0.36 (0.26)	0.98 (0.97)	0.67 (0.50)	0.95 (0.88)	0.93 (0.87)
40	0.36 (0.26)	1.00 (0.99)	1.00 (0.67)	0.95 (0.88)	0.95 (0.89)
BDG (ng/ml)					
2	0.64 (0.42)	0.91 (0.90)	0.39 (0.33)	0.97 (0.89)	0.89 (0.83)
3	0.55 (0.29)	0.95 (0.95)	0.50 (0.66)	0.96 (0.88)	0.92 (0.85)
5	0.55 (0.29)	0.98 (0.97)	0.67 (0.60)	0.96 (0.88)	0.94 (0.87)
11	0.45 (0.25)	0.99 (0.99)	0.83 (0.71)	0.95 (0.87)	0.95 (0.87)

result, the ROC curve for the GM test seemed to be better than those for the other two tests.

We previously reported that this real-time PCR for *Aspergillus* DNA was highly sensitive in vitro and with clinical samples (17): it could stably detect as few as 40 copies/ml in vitro and showed a higher sensitivity (79%) than those of the GM (58%) and BDG (67%) tests. In the present prospective analysis with consecutive patients, however, these results were not reproduced. This may be partly explained by the fact that our previous study included many retrospective samples. Furthermore, we intentionally selected IA patients and used a higher cutoff value for the GM test. Although several authors have also reported excellent sensitivity in PCR assays for IA (5, 6, 14, 34), we cannot directly compare those results with ours since there were differences in the target genes, methods of DNA extraction, starting materials, and designs of the PCR amplifications. Some form of standardization is required to make an international comparison possible. We used our real-time PCR system (GeniQ-Asper) (17) because it is most widely used in Japan. Several authors, including Loeffler et al. and Costa et al., also published excellent real-time PCR detection systems for *Aspergillus* DNA (9, 21, 26, 28), and their systems might produce superior results in the diagnosis of IA, which should be addressed in future studies.

As a diagnostic test, PCR requires more time and more complicated processing and thus costs more than the BDG and GM tests. It costs six times (15,700 yen/test) as much as the BDG and GM assays (2,700 yen/test) in Japan. A specialized laboratory as well as an expensive assay system and reagents are also required. These problems should be addressed before PCR is widely accepted as a standard screening test for IA, although it still seems to have value in making a diagnosis when a variety of clinical samples are used (20, 26, 28, 31).

The BDG test has also been widely used in Japan as a noninvasive diagnostic test for IFI. While it covers wide ranges of fungal species and may be potentially more useful as a screening test for IFI, it can cause frequent nonspecific reactions to various medical materials. Three kinds of assay systems for BDG have been developed in Japan: a chromogenic assay (FungiTec G test), β-glucan test Maruha) and a kinetic assay (β-glucan test Wako), but there is still some debate regarding their diagnostic potential. According to a sample-based analysis by Yoshida et al. (35), the chromogenic assay seems to be more sensitive (87.9 and 72.7%, respectively) than the kinetic assay but much less specific (43.3 and 75.2%, respectively) when the cutoff values recommended by the manufacturers are used. In the present study, where we used a kinetic assay, we could not obtain sufficient sensitivity even with the cutoff being maximally reduced. Furthermore, even if positive results were obtained, the positive results with the BDG test tended to occur later in the clinical course. The present result (55% sensitivity and 98% specificity) is consistent with our previous results (67% sensitivity and 84% specificity) using the chromogenic assay and also with other reports. This seems to be an inherent limitation of BDG assays

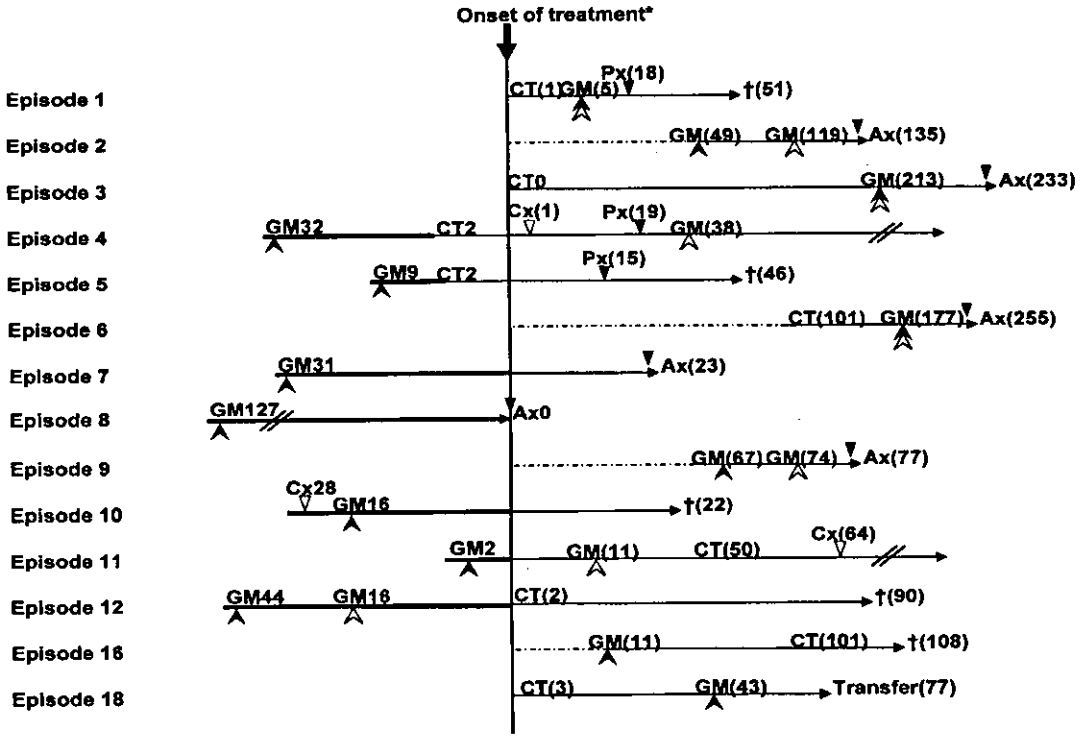

FIG. 2. Number of days from when GM assays become positive to the onset of treatment, using a threshold of 0.6 O.D.I. by method II (solid arrowheads) or 1.0 O.D.I. by method II (open arrowheads), or positive findings on CT. Open triangles indicate the date of positive culture, and solid triangles indicate when the histopathological diagnosis was made (Px, biopsy; Ax, autopsy). The values in parentheses indicate the number of days after the onset of treatment. For example, for episode 11, CT showed specific findings 50 days after the onset of treatment and the GM assay become positive 2 days before treatment. Episode numbers correspond to those in Table 2. Episodes whose GM assays did not reach the threshold are not shown. For episodes 2 and 9, a CT scan was not performed, and for episodes 7, 8, 10, 17, 19, 21, and 22, the CT findings were nonspecific and could not be used for decision-making. Each treatment was started at the discretion of the physician, taking into account various prices of clinical information, including CT findings and the results of GM assays. For Episode 8, IA was not suspected and no antifungal agent was administered. Therefore, the date of death was used instead of the date of treatment onset.

for the diagnosis of IA, although they show a very high sensitivity and specificity for candidiasis (25).

The diagnostic potential of double-sandwich ELISA for GM has been repeatedly validated in recent large-scale studies (15, 22). However, a direct comparison of the results of different studies, including ours, is not always easy and in fact can be quite difficult or impractical. Many factors can influence the apparent sensitivity and specificity and of course the PPV and NPV. Therefore, the important point is the way in which these results should be interpreted, and this depends on the objective and design of each study. From this perspective, our results are comparable to those of Maertens et al. (22) but in contrast to those of Herbrecht et al. (15). The latter addressed principally the diagnostic potential of the GM test in the presence of an unknown neutropenic fever or some respiratory signs and symptoms in cancer patients. On the other hand, in our study as well as in that of Maertens et al., the principal concern was the potential of the test in serial screenings with multiple measurements throughout the entire period of hematology care. For example, the mean numbers of measurements per episode in our study and that of Maertens et al. (8.3 and 11.2 per episode, respectively, with GM measured weekly) are significantly different from that in the study of Herbrecht et al. (5.5 per episode, with GM measured daily or weekly), consistent with the study designs. The difference becomes more prominent for proven IA episodes (17.3 and 19 versus 6.8). The differences in the mean number and timing of measurements clearly affect the apparent sensitivity and specificity of the studies. Hence, the apparent statistical values obtained by Herbrecht et al. are expected to be lower than ours and those of

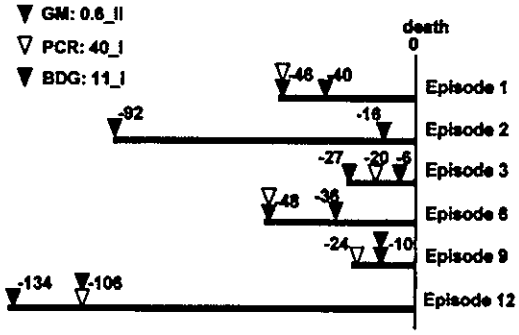

FIG. 3. Number of days before death that each test gave positive results. Solid triangles indicate the date when GM became positive, using a threshold of 0.6 O.D.I. by method II; open triangles indicate the date when PCR exceeded a cutoff value of 40 copies/ml; and shaded triangles indicate the date when the BDG test exceeded a cutoff value of 11 ng/ml, by method I. In episode 2, PCR never exceeded the cutoff value. Episode numbers correspond to those in Table 2.

Maertens et al., but they should provide a better approximation of the corresponding sample-based statistics, even though the patient population was more heterogeneous.

According to the ROC analysis of double-sandwich ELISA, the conventionally used cutoff seems to be too high: our recommendation is 0.6 O.D.I., and two consecutive positive results should be taken into consideration. With these new criteria, the GM test showed an excellent chronological profile. It gave the first positive diagnostic result in 9 of 14 GM-positive IA episodes and in 5 of 9 IA or possible IFI episodes where both CT and GM were positive. It preceded the initiation of empiric or definitive antifungal therapy in seven episodes. Using the novel criteria, positivity was ascertained a median of 10 days before conventional positivity was noted, and in six cases the GM test gave positive results only with the novel criteria. These chronological advantages were not observed with a threshold of 1.0 O.D.I. by method II: for episodes 5, 7, 8, and 10, the GM assay did not become positive; for episode 4, the GM assay exceeded the criteria 38 days after the onset of treatment; for episode 12, the GM assay gave positive results 16 days before the onset of treatment. According to the high PPV with the novel cutoff criteria (0.55 for proven or probable IA and 0.48 for proven, probable, or possible IFI) and the early timing of its positivity, we could have initiated antifungal therapy in a preemptive manner for episodes 4, 5, 7, 8, 10, 11, and 12.

Our result does not justify a discontinuation or moratorium of empiric antifungal treatment based only on a single negative result in the face of an impending threat of IA. It should be stressed that the extremely high NPVs provided here are episode-based calculations. Sample-based NPVs should be much lower, especially when patients are at high risk. We could not exclude a possibility of other IFI. Similarly, PPV does not always represent the probability of currently having IA but, rather, predicts the probability that the subject has or will have IA. In addition, while there was a sufficient number of no-IA episodes in this study to permit reliable estimations of specificity and NPV, there is much uncertainty regarding the estimations of the absolute values of sensitivity and PPV because of the small number of IA patients.

REFERENCES

1. **Andreas, S., S. Heindl, C. Wattky, K. Moller, and R. Ruchel.** 2000. Diagnosis of pulmonary aspergillosis using optical brighteners. Eur. Respir. J. **15**:407–411.
2. **Ascioglu, S., J. H. Rex, B. de Pauw, J. E. Bennett, J. Bille, F. Crokaert, D. W. Denning, J. P. Donnelly, J. E. Edwards, Z. Erjavec, D. Fiere, O. Lortholary, J. Maertens, J. F. Meis, T. F. Patterson, J. Ritter, D. Selleslag, P. M. Shah, D. A. Stevens, and T. J. Walsh.** 2002. Defining opportunistic invasive fungal infections in immunocompromised patients with cancer and hematopoietic stem cell transplants: an international consensus. Clin. Infect. Dis. **34**:7–14.
3. **Becker, M. J., S. de Marie, D. Willemse, H. A. Verbrugh, and I. A. Bakker-Woudenberg.** 2000. Quantitative galactomannan detection is superior to PCR in diagnosing and monitoring invasive pulmonary aspergillosis in an experimental rat model. J. Clin. Microbiol. **38**:1434–1438.
4. **Bowden, R., P. Chandrasekar, M. H. White, X. Li, L. Pietrelli, M. Gurwith, J. A. van Burik, M. Laverdiere, S. Safrin, and J. R. Wingard.** 2002. A double-blind, randomized, controlled trial of amphotericin B colloidal dispersion versus amphotericin B for treatment of invasive aspergillosis in immunocompromised patients. Clin. Infect. Dis. **35**:359–366.
5. **Bretagne, S., J. M. Costa, E. Bart-Delabesse, N. Dhedin, C. Rieux, and C. Cordonnier.** 1998. Comparison of serum galactomannan antigen detection and competitive polymerase chain reaction for diagnosing invasive aspergillosis. Clin. Infect. Dis. **26**:1407–1412.
6. **Buchheidt, D., C. Baust, H. Skladny, J. Ritter, T. Suedhoff, M. Baldus, W. Seifarth, C. Leib-Moesch, and R. Hehlmann.** 2001. Detection of *Aspergillus* species in blood and bronchoalveolar lavage samples from immunocompromised patients by means of 2-step polymerase chain reaction: clinical results. Clin. Infect. Dis. **33**:428–435.
7. **Caillot, D., O. Casasnovas, A. Bernard, J. F. Couaillier, C. Durand, B. Cuisenier, E. Solary, F. Piard, T. Petrella, A. Bonnin, G. Couillault, M. Dumas, and H. Guy.** 1997. Improved management of invasive pulmonary aspergillosis in neutropenic patients using early thoracic computed tomographic scan and surgery. J. Clin. Oncol. **15**:139–147.
8. **Caillot, D., J. F. Couaillier, A. Bernard, O. Casasnovas, D. W. Denning, L. Mannone, J. Lopez, G. Couillault, F. Piard, O. Vagner, and H. Guy.** 2001. Increasing volume and changing characteristics of invasive pulmonary aspergillosis on sequential thoracic computed tomography scans in patients with neutropenia. J. Clin. Oncol. **19**:253–259.
9. **Costa, C., J. M. Costa, C. Desterke, F. Botterel, C. Cordonnier, and S. Bretagne.** 2002. Real-time PCR coupled with automated DNA extraction and detection of galactomannan antigen in serum by enzyme-linked immunosorbent assay for diagnosis of invasive aspergillosis. J. Clin. Microbiol. **40**:2224–2227.
10. **Denning, D. W.** 1998. Invasive aspergillosis. Clin. Infect. Dis. **26**:781–803.
11. **Denning, D. W.** 1996. Therapeutic outcome in invasive aspergillosis. Clin. Infect. Dis. **23**:608–615.
12. **Einsele, H., H. Hebart, G. Roller, J. Loffler, I. Rothenhofer, C. A. Muller, R. A. Bowden, J. van Burik, D. Engelhard, L. Kanz, and U. Schumacher.** 1997. Detection and identification of fungal pathogens in blood by using molecular probes. J. Clin. Microbiol. **35**:1353–1360.
13. **Hanley, J. A., and B. J. McNeil.** 1983. A method of comparing the areas under receiver operating characteristic curves derived from the same cases. Radiology **148**:839–843.
14. **Hebart, H., J. Loffler, C. Meisner, F. Serey, D. Schmidt, A. Bohme, H. Martin, A. Engel, D. Bunje, W. V. Kern, U. Schumacher, L. Kanz, and H. Einsele.** 2000. Early detection of aspergillus infection after allogeneic stem cell transplantation by polymerase chain reaction screening. J. Infect. Dis. **181**:1713–1719.
15. **Herbrecht, R., V. Letscher-Bru, C. Oprea, B. Lioure, J. Waller, F. Campos, O. Villard, K. L. Liu, S. Natarajan-Ame, P. Lutz, P. Dufour, J. P. Bergerat, and E. Candolfi.** 2002. Aspergillus galactomannan detection in the diagnosis of invasive aspergillosis in cancer patients. J. Clin. Oncol. **20**:1898–1906.
16. **Hughes, W. T., D. Armstrong, G. P. Bodey, A. E. Brown, J. E. Edwards, R. Feld, P. Pizzo, K. V. Rolston, J. L. Shenep, and L. S. Young.** 1997. 1997 guidelines for the use of antimicrobial agents in neutropenic patients with unexplained fever. Infectious Diseases Society of America. Clin. Infect. Dis. **25**:551–573.
17. **Kami, M., T. Fukui, S. Ogawa, Y. Kazuyama, U. Machida, Y. Tanaka, Y. Kanda, T. Kashima, Y. Yamazaki, T. Hamaki, S. Mori, H. Akiyama, Y. Mutou, H. Sakamaki, K. Osumi, S. Kimura, and H. Hirai.** 2001. Use of real-time PCR on blood samples for diagnosis of invasive aspergillosis. Clin. Infect. Dis. **33**:1504–1512.
18. **Kami, M., Y. Tanaka, Y. Kanda, S. Ogawa, T. Masumoto, K. Ohtomo, T. Matsumura, T. Saito, U. Machida, T. Kashima, and H. Hirai.** 2000. Computed tomographic scan of the chest, latex agglutination test and plasma (1AE3)-beta-D-glucan assay in early diagnosis of invasive pulmonary aspergillosis: a prospective study of 215 patients. Haematologica **85**:745–752.
19. **Kawamura, S., S. Maesaki, T. Noda, Y. Hirakata, K. Tomono, T. Tashiro, and S. Kohno.** 1999. Comparison between PCR and detection of antigen in sera for diagnosis of pulmonary aspergillosis. J. Clin. Microbiol. **37**:218–220.
20. **Kawazu, M., Y. Kanda, S. Goyama, M. Takeshita, Y. Nannya, M. Niino, Y. Komeno, T. Nakamoto, M. Kurokawa, S. Tsujino, S. Ogawa, K. Aoki, S. Chiba, T. Motokura, N. Ohishi, and H. Hirai.** 2003. Rapid diagnosis of invasive pulmonary aspergillosis by quantitative polymerase chain reaction using bronchial lavage fluid. Am. J. Hematol. **72**:27–30.
21. **Loeffler, J., N. Henke, H. Hebart, D. Schmidt, L. Hagmeyer, U. Schumacher, and H. Einsele.** 2000. Quantification of fungal DNA by using fluorescence resonance energy transfer and the light cycler system. J. Clin. Microbiol. **38**:586–590.
22. **Maertens, J., J. Verhaegen, K. Lagrou, J. Van Eldere, and M. Boogaerts.** 2001. Screening for circulating galactomannan as a noninvasive diagnostic tool for invasive aspergillosis in prolonged neutropenic patients and stem cell transplantation recipients: a prospective validation. Blood **97**:1604–1610.
23. **Mori, T., H. Ikemoto, M. Matsumura, M. Yoshida, K. Inada, S. Endo, A. Ito, S. Watanabe, H. Yamaguchi, M. Mitsuya, M. Kodama, T. Tani, T. Yokota, T. Kobayashi, J. Kambayashi, T. Nakamura, T. Masaoka, H. Teshima, T. Yoshinaga, S. Kohno, K. Hara, and S. Miyazaki.** 1997. Evaluation of plasma (1→3)-beta-D-glucan measurement by the kinetic turbidimetric *Limulus* test for the clinical diagnosis of mycotic infections. Eur. J. Clin. Chem. Clin. Biochem. **35**:553–560.
24. **Nakai, T., J. Uno, K. Otomo, F. Ikeda, S. Tawara, T. Goto, K. Nishimura, and M. Miyaji.** 2002. In vitro activity of FK463, a novel lipopeptide antifungal agent, against a variety of clinically important molds. Chemotherapy **48**:78–81.
25. **Obayashi, T., M. Yoshida, T. Mori, H. Goto, A. Yasuoka, H. Iwasaki, H. Teshima, S. Kohno, A. Horiuchi, A. Ito, et al.** 1995. Plasma (1→3)-beta-D-glucan measurement in diagnosis of invasive deep mycosis and fungal febrile episodes. Lancet **345**:17–20.

26. **Rantakokko-Jalava, K., S. Laaksonen, J. Issakainen, J. Vauras, J. Nikoskelainen, M. K. Viljanen, and J. Salonen.** 2003. Semiquantitative detection by real-time PCR of *Aspergillus fumigatus* in bronchoalveolar lavage fluids and tissue biopsy specimens from patients with invasive aspergillosis. J. Clin. Microbiol. **41**:4304–4311.
27. **Salonen, J., O. P. Lehtonen, M. R. Terasjarvi, and J. Nikoskelainen.** 2000. Aspergillus antigen in serum, urine and bronchoalveolar lavage specimens of neutropenic patients in relation to clinical outcome. Scand. J. Infect. Dis. **32**:485–490.
28. **Sanguinetti, M., B. Posteraro, L. Pagano, G. Pagliari, L. Fianchi, L. Mele, M. La Sorda, A. Franco, and G. Fadda.** 2003. Comparison of real-time PCR, conventional PCR, and galactomannan antigen detection by enzyme-linked immunosorbent assay using bronchoalveolar lavage fluid samples from hematology patients for diagnosis of invasive pulmonary aspergillosis. J. Clin. Microbiol. **41**:3922–3925.
29. **Stone, E. A., H. B. Fung, and H. L. Kirschenbaum.** 2002. Caspofungin: an echinocandin antifungal agent. Clin. Ther. **24**:351–377; discussion, 329.
30. **Stynen, D., A. Goris, J. Sarfati, and J. P. Latge.** 1995. A new sensitive sandwich enzyme-linked immunosorbent assay to detect galactofuran in patients with invasive aspergillosis. J. Clin. Microbiol. **33**:497–500.
31. **Tang, C. M., D. W. Holden, A. Aufauvre-Brown, and J. Cohen.** 1993. The detection of *Aspergillus* spp. by the polymerase chain reaction and its evaluation in bronchoalveolar lavage fluid. Am. Rev. Respir. Dis. **148**:1313–1317.
32. **Verweij, P. E., D. Stynen, A. J. Rijs, B. E. de Pauw, J. A. Hoogkamp-Korstanje, and J. F. Meis.** 1995. Sandwich enzyme-linked immunosorbent assay compared with Pastorex latex agglutination test for diagnosing invasive aspergillosis in immunocompromised patients. J. Clin. Microbiol. **33**:1912–1914.
33. **Walsh, T. J., P. Pappas, D. J. Winston, H. M. Lazarus, F. Petersen, J. Raffalli, S. Yanovich, P. Stiff, R. Greenberg, G. Donowitz, M. Schuster, A. Reboli, J. Wingard, C. Arndt, J. Reinhardt, S. Hadley, R. Finberg, M. Laverdiere, J. Perfect, G. Garber, G. Fioritoni, E. Anaissie, and J. Lee.** 2002. Voriconazole compared with liposomal amphotericin B for empirical antifungal therapy in patients with neutropenia and persistent fever. N. Engl. J. Med. **346**:225–234.
34. **Yamakami, Y., A. Hashimoto, I. Tokimatsu, and M. Nasu.** 1996. PCR detection of DNA specific for *Aspergillus* species in serum of patients with invasive aspergillosis. J. Clin. Microbiol. **34**:2464–2468.
35. **Yoshida, K., Y. Niki, H. Mitekura, M. Nakajima, H. Kawane, and T. Matsushima.** 2001. A discrepancy in the values of serum (1–3)-beta-D-glucan measured by two kits using different methods. Nippon Ishinkin Gakkai Zasshi **42**:237–242. (In Japanese.)

The transcriptionally active form of AML1 is required for hematopoietic rescue of the *AML1*-deficient embryonic para-aortic splanchnopleural (P-Sp) region

Susumu Goyama, Yuko Yamaguchi, Yoichi Imai, Masahito Kawazu, Masahiro Nakagawa, Takashi Asai, Keiki Kumano, Kinuko Mitani, Seishi Ogawa, Shigeru Chiba, Mineo Kurokawa, and Hisamaru Hirai

Acute myelogenous leukemia 1 (AML1; runt-related transcription factor 1 [Runx1]) is a member of Runx transcription factors and is essential for definitive hematopoiesis. Although AML1 possesses several subdomains of defined biochemical functions, the physiologic relevance of each subdomain to hematopoietic development has been poorly understood. Recently, the consequence of carboxy-terminal truncation in AML1 was analyzed by the hematopoietic rescue assay of *AML1*-deficient mouse embryonic stem cells using the gene knock-in approach. Nonetheless, a role for specific internal domains, as well as for mutations found in a human disease, of AML1 remains to be elucidated. In this study, we established an experimental system to efficiently evaluate the hematopoietic potential of AML1 using a coculture system of the murine embryonic para-aortic splanchnopleural (P-Sp) region with a stromal cell line, OP9. In this system, the hematopoietic defect of *AML1*-deficient P-Sp can be rescued by expressing AML1 with retroviral infection. By analysis of AML1 mutants, we demonstrated that the hematopoietic potential of AML1 was closely related to its transcriptional activity. Furthermore, we showed that other Runx transcription factors, Runx2/AML3 or Runx3/AML2, could rescue the hematopoietic defect of *AML1*-deficient P-Sp. Thus, this experimental system will become a valuable tool to analyze the physiologic function and domain contribution of Runx proteins in hematopoiesis. (Blood. 2004;104:3558-3564)

Introduction

Acute myelogenous leukemia 1 (AML1)/runt-related transcription factor 1 (Runx1) belongs to a family of transcriptional regulators called Runx, which contain a conserved 128–amino acid Runt domain responsible for sequence-specific DNA binding.[1] Runx proteins make heterodimeric complexes with a partner protein, CBFβ/PEBP2β (core-binding factor β/polyomavirus enhancer–binding protein 2β),[2-4] and this association is essential for its biologic activity.[5-7] There are 3 known mammalian Runx family members: AML1/Runx1, Runx2/AML3, and Runx3/AML2. Typically, Runx functions as a transcriptional activator of target gene expression. Under some conditions, however, it can repress the transcription of specific genes.

AML1 was originally identified on chromosome 21 as the gene that is disrupted in the (8;21)(q22;q22) translocation, which is one of the most frequent chromosome abnormalities associated with human AML.[8,9] Subsequently, AML1 was shown to be one of the most frequent targets of leukemia-associated gene aberrations.[10,11] Moreover, somatic point mutations of the *AML1* gene were also demonstrated in patients with AML and myelodysplastic syndrome (MDS).[12-14] In addition to a role in leukemic transformation, gene-targeting studies in mice have demonstrated that AML1 is essential for early development of definitive hematopoiesis. *AML1*-deficient embryos develop through the yolk sac stage but die around 12 to 13 days of gestation following complete block of fetal liver hematopoiesis.[15,16]

AML1 includes at least 3 alternative splicing forms: AML1a, AML1b, and AML1c.[17] In AML1b and AML1c, the carboxy (C)–terminal to the Runt domain lies in a region that contains sequences of defined biochemical functions, which are absent in AML1a. Several functional domains have been identified in the C-terminal half, such as *trans*-activation domain,[18,19] *trans*-repression domain,[20] and VWRPY motif.[21-23]

During vertebrate embryogenesis, hematopoietic development consists of 2 distinct waves of discrete cellular components known as primitive and definitive hematopoiesis.[24] In mice, the first wave of primitive hematopoiesis, which consists predominantly of a large and nucleated erythroid cell, emerges in the yolk sac at 7.5 embryonic days after coitus (dpc). Then, primitive hematopoiesis begins to be replaced around 9.5 dpc by definitive hematopoiesis, generally described as the second wave. Progenitors for definitive hematopoiesis originate from para-aortic splanchnopleural (P-Sp) region at 7.5 to 9.5 dpc,[25,26] and long-term repopulating hematopoietic stem cells (LTR-HSCs) that can reconstitute adult mice appear in the aorta-gonad-mesonephros (AGM) at 10.5 to 11.5 dpc.[27,28] These cells subsequently colonize the fetal liver, where they expand and differentiate. Active sites for definitive hematopoiesis

From the Departments of Hematology/Oncology and Regeneration Medicine for Hematopoiesis, Graduate School of Medicine, University of Tokyo, Tokyo, Japan; Department of Cell Therapy/Transplantation Medicine, University of Tokyo Hospital, University of Tokyo, Tokyo, Japan; and Department of Hematology, Dokkyo University School of Medicine, Tochigi, Japan.

Submitted April 22, 2004; accepted July 6, 2004. Prepublished online as *Blood* First Edition Paper, July 22, 2004; DOI 10.1182/blood-2004-04-1535.

Supported in part by a Grant-in-Aid for Scientific Research from the Japan Society for the Promotion of Science and by Health and Labour Sciences Research grants from the Ministry of Health, Labour, and Welfare.

An Inside *Blood* analysis of this article appears in the front of this issue.

Reprints: Mineo Kurokawa, Department of Hematology & Oncology, Graduate School of Medicine, University of Tokyo, 7-3-1 Hongo, Bunkyo-ku, Tokyo 113-8655, Japan; e-mail: kurokawa-tky@umin.ac.jp.

The publication costs of this article were defrayed in part by page charge payment. Therefore, and solely to indicate this fact, this article is hereby marked "advertisement" in accordance with 18 U.S.C. section 1734.

are transferred to bone marrow and spleen prior to birth and function throughout life within these organs. Recent studies have shown that AML1 is expressed in the hematopoietic cell clusters within the P-Sp/AGM region and *AML1*-deficient embryos are devoid of these hematopoietic clusters.[29-32]

The hematopoietic defect of *AML1*-deficient mice could be replicated in vitro by several culture systems, including the P-Sp/AGM culture[33,34] and the embryonic stem (ES) cell culture.[35] In these systems, hematopoietic cells are generated in wild-type cultures but not in *AML1*-deficient cultures. Recently, a gene knock-in approach was used to demonstrate rescue in vivo of hematopoiesis from the *AML1*-deficient ES cells.[35,36] This hematopoietic rescue requires the *trans*-activation domain of AML1 but not the C-terminal *trans*-repression subdomain. However, no report has elucidated roles for specific internal domains or disease-related mutations of AML1 in hematopoiesis.

In the present study, we used a coculture system of cells derived from the P-Sp region with a layer of a stromal cell line, OP9, in which hematopoietic cell development of various lineages is efficiently induced.[37] The cultured P-Sp–derived cells show a significant colony-forming activity in semisolid culture with appropriate cytokines, as well as distinct surface expression of hematopoietic markers. In this culture system, *AML1*-deficient P-Sp–derived cells failed to show any hematopoietic activity. This defect was efficiently rescued by reactivating AML1 by retroviral-mediated expression. Using this system, we then examined a hematopoietic potential of a series of AML1 mutants and demonstrated that the hematopoietic rescue of *AML1*-deficient P-Sp regions require transcriptionally active forms of AML1. We also showed that enforced expression of other Runx transcription factors, Runx2/AML3 or Runx3/AML2, could rescue the hematopoietic defect of *AML1*-deficient P-Sp regions. These results provide evidence that transcriptional activity of AML1 is essential for hematopoietic development from P-Sp regions. In addition, this coculture system makes a useful method to determine functional consequences of AML1 on its hematopoietic potential.

Materials and methods

Mice and embryos

AML1-deficient mice were generated as described previously[38] and were crossed onto the C57BL/6 background. To generate embryos, timed matings were set up between $AML1^{+/-}$ males and $AML1^{+/-}$ females. The time at midday (12:00) was taken to be 0.5 dpc for the plugged mice.

In vitro P-Sp culture

P-Sp culture was performed as described previously[39] with a minor modification. In brief, isolated P-Sp regions of 9.5 dpc embryos were dissociated by incubation with 250 U/mL dispase (Godo Shusei, Tokyo, Japan) for 20 minutes and cell dissociation buffer (Gibco BRL, Carlsbad, CA) for 20 minutes at 37°C, washed once in phosphate-buffered saline (PBS), followed by vigorous pipetting. Approximately 5×10^4 P-Sp–derived cells were suspended in 300 μL serum-free StemPro media (Life Technologies, Gaithersburg, MD) supplemented with 50 ng/mL stem cell factor (SCF), 5 ng/mL interleukin (IL3; gifts from Kirin Brewery, Takasaki, Japan), and 10 ng/mL murine oncostatin M (R&D Systems, Minneapolis, MN). Single-cell suspensions were seeded on preplated OP-9 stromal cells in the 24-well plate, followed by incubation at 37°C.

Plasmid construction

The cDNAs of human AML1a, AML1b, and various AML1 mutants were subcloned as *Eco*RI-*Eco*RI fragments into the retrovirus vector pMY/ internal ribosomal entry site–enhanced green fluorescent protein (IRES-EGFP; pMY/IG).[40] C-terminal deletion mutants of AML1b, AML1b-R139G, AML1b-S249/266A, and AML1b-K24/43R were constructed as described previously.[13,41-43] For construction of AML1bΔ(205-332), we deleted the *Pvu*II-*Bst*PI fragment from AML1b, filled the resultant plasmid with a Klenow fragment, and religated it. AML1bΔ(181-210) was created by polymerase chain reaction (PCR) with the insertion of a *Bgl*II restriction site to join the fragments. Flag-tagged human Runx2/AML3 cDNA was inserted into the *Bam*HI and the *Eco*RI restriction sites of pMYs/IRES-EGFP (pMYs/IG).[40] Flag-tagged human Runx3/AML2 cDNA was inserted into the *Sac*II and the *Xho*I sites of the same vector.

Retroviral transduction

Plat-E packaging cells[44] (2×10^6) were transiently transfected with 3 μg of AML1, Runx2/AML3, Runx3/AML2, or AML1 mutants; mixed with 9 μL of FuGENE6 (Roche Molecular Biochemicals, Indianapolis, IN); followed by incubation at 37°C. Supernatant containing retrovirus was collected 48 hours after transfection and used immediately for infection. Retroviral transduction to the cells derived from *AML1*-deficient P-Sp regions was performed as described previously with minor modification.[45] In brief, the viral supernatant was added to the P-Sp culture together with 10 μg/mL Polybrene (Sigma, St Louis, MO). After 72 hours of incubation, virus-containing medium was replaced by standard culture medium. The cells were incubated for another 10 days and processed for analysis. To confirm the expression of Runx proteins, NIH3T3 cells were also infected with the same viral supernatants. The number of retrovirus-infected cells was evaluated by the expression of green fluorescent protein (GFP).

Colony-forming cell (CFC) assay

The nonadherent or semiadherent cells rescued from *AML1*-deficient P-Sp regions were used for CFC assay. Cells (6×10^4) were plated into MethoCult3434 medium (StemCell Technologies, Vancouver, BC, Canada) and cultured in a 5% CO_2 incubator at 37°C. Colony types were determined at day 7 by morphologic appearance and by Wright-Giemsa staining of each colony.

Flow cytometry analysis

Flow cytometry analysis was performed in a FACScalibur with the Cellquest program (Becton Dickinson, San Jose, CA) after addition of propidium iodide to exclude dead cells. For surface staining, cell suspensions collected from the P-Sp cultures were incubated on ice for 30 minutes in the presence of various mixtures of labeled monoclonal antibodies. The monoclonal antibodies used were phycoerythrin (PE)–conjugated anti–granulocyte 1 (anti-Gr1), anti–macrophage antigen 1 (anti-Mac1), anti–stem cell antigen 1 (anti-Sca1), allophycocyanin (APC)–conjugated anti-CD45, anti–c-Kit, and biotin-conjugated anti-CD34. Biotinylated antibodies were then counterstained with PE- or APC-conjugated streptavidin. Isotype-matched antibodies conjugated with the appropriate fluorochrome were used as negative controls.

Western blot analysis

Retrovirus-infected NIH3T3 cells were lysed in radioimmunoprecipitation assay (RIPA) buffer.[41] Whole-cell lysates containing 100 μg of proteins were subjected to sodium dodecyl sulfate–polyacrylamide gel electrophoresis (SDS-PAGE) and transferred to a polyvinylidene difluoride membrane (Immobilon; Millipore, Bedford, MA). The membrane was blocked with 10% skim milk, treated with anti-AML1 (PC284L; Oncogene, Cambridge, MA) or anti-Flag (M2; Sigma), washed, and reacted with the rabbit anti–immunoglobulin G (anti-IgG) antibody coupled to horseradish peroxidase. The blot was visualized using the enhanced chemiluminescence (ECL) system (Amersham Pharmacia Biotech, Piscataway, NJ).

Results

Retroviral expression of AML1 rescues hematopoiesis by *AML1*-deficient P-Sp region

AML1-deficient mice die in midgestation as a result of a complete block in fetal liver hematopoiesis, indicating the strict in vivo requirement of AML1 in definitive hematopoiesis. Consistently, the primary culture system of the P-Sp region has demonstrated that the failure of hematopoiesis in the fetal liver is preceded by a hematopoietic defect in the P-Sp region, from which the development of hematopoietic cells was never detected in *AML1*-deficient embryos.[34,45] When the cells isolated from wild-type P-Sp regions at 9.5 dpc were cocultured with OP9 stromal cells, small and round-shaped nonadherent cells were produced in 5 days (Figure 1A). These cells were thought to represent a hematopoietic cell population of various lineages because they expressed hematopoietic cell surface markers and generated hematopoietic cell colonies when plated into a semisolid culture (Figure 2; data not shown). In contrast, the cells from *AML1*-deficient P-Sp regions failed to develop any hematopoietic cells (Figure 1B), which coincides with the notion that AML1 is a prerequisite for hematopoietic cell production in the P-Sp region. Thus, AML1-dependent hematopoiesis could be recapitulated in vitro, and we went on further to examine whether reactivation of a transcriptionally active form of AML1 can rescue this hematopoietic defect. First, by packaging the pMY/IG-AML1b in Plat-E cells, we generated the AML1b-IRES-GFP retrovirus that expresses AML1b and GFP. Then we infected the cells derived from the *AML1*-deficient P-Sp region with the AML1b-IRES-GFP retrovirus and cultured for an additional 10 days. Interestingly, AML1b-infected cultures generated numerous small and round cells with a nonadherent property (Figure 1C). In contrast, cultures infected with the empty vector (control) produced no such cells (Figure 1D). These nonadherent cells were morphologically indistinguishable from the hematopoietic cells generated from the wild-type P-Sp cells and proliferated continuously for more than 30 days. These results suggest that lack of P-Sp hematopoiesis can be complemented by retrovirus-mediated reactivation of AML1 in this culture system.

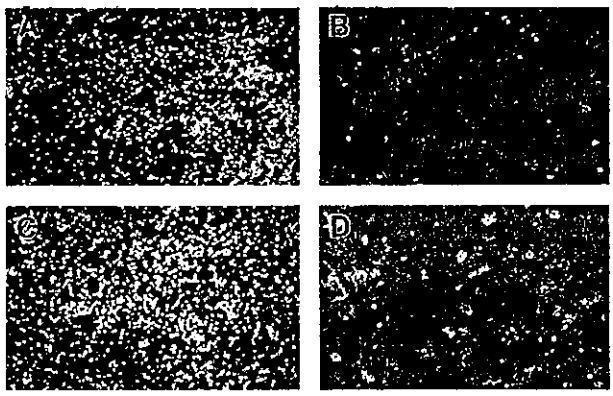

Figure 1. Retroviral expression of AML1b rescues hematopoiesis from *AML1*-deficient P-Sp regions. Photographs were taken with a Nikon Eclipse TE2000-U (Nikon Sankei, Tokyo, Japan) at a magnification of × 100 after 5 days of culture (A-B) and 14 days of culture (C-D). (A) Hematopoietic cells emerged at day 5 from wild-type P-Sp regions. (B) No hematopoietic cells were observed in the culture of *AML1*-deficient P-Sp regions, showing only the background of OP9 cells. (C) AML1b-transduced P-Sp regions from an *AML1*-deficient embryo generated numerous round, nonadherent, or semiadherent cells. (D) A control culture infected with mock virus failed to generate any hematopoietic cells.

Rescued cells retain the features of hematopoietic cells

In the previous study, Mukouyama et al[45] described that the retroviral transfer of AML1 into the *AML1*-deficient P-Sp region gave rise to the production of small and round cells in the culture with an appropriate combination of cytokines. However, under their experimental condition in which no stromal cell layer was employed, the recovered cells showed neither CFC activity nor expression of hematopoietic cell surface markers, such as CD45 and c-Kit, which indicates that the rescue of the hematopoietic defect is incomplete, if it occurs at all. To determine whether the nonadherent cells recovered under our experimental condition retain the features of hematopoietic cells, we examined CFC activity and surface markers of those cells, both of which are distinctly detected in wild-type P-Sp–derived cells in our coculture system. On the 10th day of culture, the nonadherent cells were collected and seeded into a semisolid medium. As shown in Figure 3, these cells generated a number of mixed, granulocyte/macrophage, and erythroid colonies, indicating that the recovered cells should contain various types of CFCs, possibly including definitive lineages. In addition, the flow cytometric analysis revealed that the rescued cells expressed hematopoietic cell surface markers, such as a marker of hematopoietic cells, CD45; myeloid markers Gr1/Mac1; and markers of hematopoietic progenitors c-Kit, Sca1, and CD34 (Figure 2). Their expression profiles were nearly identical to those of hematopoietic cells generated from the wild-type P-Sp cells (Figure 2).

Thus, in contrast to the previous report,[45] we found that the nonadherent cells derived from *AML1*-deficient P-Sp regions in our culture system retained the features of hematopoietic cells that are indistinguishable from those of wild-type P-Sp–derived cells. It is, thus, likely that seeding onto OP9 stromal cells may provide a more favorable environment for production of hematopoietic cells from P-Sp regions and/or the expansion of P-Sp–derived hematopoietic cells.

Hematopoietic potential of AML1 mutants

Using this experimental system, we then analyzed the hematopoietic potential of various AML1 mutants (Figure 4). We generated retroviruses that express a variety of AML1 mutants, including serial C-terminal truncation, deletion of functional domains, and substitution of specific residues. NIH3T3 cells were infected with these viruses and the titer of the retroviruses was evaluated by flow cytometric measurement of GFP-positive NIH3T3 cells (Figure 5A). Coincidently, retrovirus-mediated expression of each mutant in infected cells was confirmed by Western blotting (Figure 5B).

Among those mutants, we first used a series of C-terminal deletion mutants including AML1a and examined their hematopoietic potential by delivering them into the *AML1*-deficient P-Sp region in our coculture system. AML1bΔ444 and AML1bΔ397, which possess the *trans*-activation subdomain, retained the ability to rescue the hematopoietic defect of the *AML1*-deficient P-Sp region (Figure 6A-B). In contrast, AML1bΔ335, AML1bΔ288, and AML1a, which lack the *trans*-activation domain, failed to produce any hematopoietic cells (Figure 6C-E). In addition, AML1bΔ(205-332), which retains the C-terminal region but lacks a half of the activation domain, has also lost the hematopoietic potential (Figure 6G). Thus, consistent with the observation in the previous report,[35] in vitro hematopoietic rescue requires the *trans*-activation domain of AML1, whereas the C-terminal repression domain including VWRPY motif is dispensable for this function.

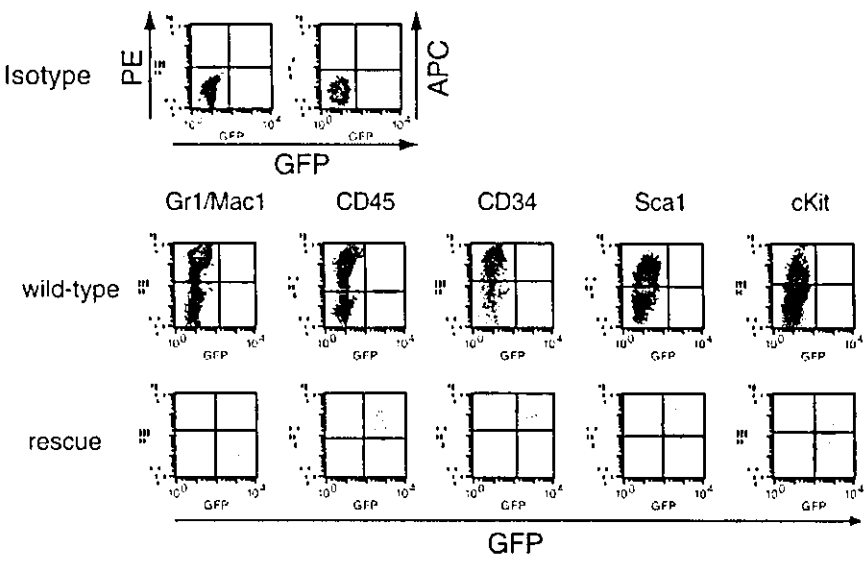

Figure 2. Expression of the hematopoietic markers on the rescued cells from *AML1*-deficient P-Sp culture. Flow cytometric profiles of the cells stained with antibodies against Gr1/Mac1, CD45, CD34, Sca1, and c-Kit. Note that the rescued cells from *AML1*-deficient P-Sp regions are GFP-positive and express various hematopoietic cell surface markers. Flow cytometric profiles of the rescued cells are similar to those of hematopoietic cells in wild-type P-Sp culture. GFP intensity (marking retrovirally transduced cells) is plotted on the x-axis and intensity of counterstaining of hematopoietic surface markers is plotted on the y-axis. Isotype-matched control staining of the hematopoietic cells from wild-type P-Sp regions is also shown.

The Runt domain of AML1 is essential for both DNA binding and heterodimerization with CBFβ, but its role in hematopoietic development has not yet been directly investigated. Therefore, we next examined the hematopoietic potential of AML1bΔRD, a deletion mutant that lacks the Runt domain and is defective for both DNA binding and heterodimerization with CBFβ. As shown in Figure 6F, AML1bΔRD could not rescue hematopoiesis from *AML1*-deficient P-Sp regions, indicating an essential role for the Runt domain in the hematopoietic potential of AML1. To elucidate more explicitly a role of DNA binding of AML1, we used AML1b-R139G, a mutant isolated from a patient with MDS, which harbors point mutation causing substitution of Arg139 in the Runt domain with Gly.[13] The DNA-binding ability is severely impaired in AML1b-R139G, whereas heterodimerization with CBFβ is spared. As shown in Figure 6I, AML1b-R139G also failed to show any hematopoietic potential. These results indicate that DNA binding of AML1 through the Runt domain is also indispensable for in vitro hematopoietic rescue of the *AML1*-deficient P-Sp region.

Among corepressors that are recruited by AML1 is mSin3A, which may contribute to AML1-mediated repression of gene transcription, as well as to intracellular stability of AML1.[20,46] Indeed, the AML1 mutant that cannot interact with mSin3A [AML1bΔ(181-210)] is defective for repression of the *p21* promoter in the in vitro transcription response assay. Posttranscriptional modification is also one of the important mechanisms that regulate AML1 function.[42,43] For example, transcriptional activity of AML1 is enhanced by extracellular signal-regulated kinase (ERK)–dependent phosphorylation on Ser249 and Ser266, whereas p300-mediated acetylation on Lys24 and Lys43 augments DNA binding of AML1. To clarify roles of these regulatory mechanisms in the hematopoietic potential of AML1, we used 3 types of AML1 mutants: AML1bΔ(181-210), AML1b-S249/266A, and AML1b-K24/43R. AML1bΔ(181-210) is an internal deletion mutant that lacks the binding domain for the mSin3A.[20] In AML1b-S249/266A, the 2 target serines for ERK-mediated phosphorylation were replaced with alanines, which results in lack of ERK-induced

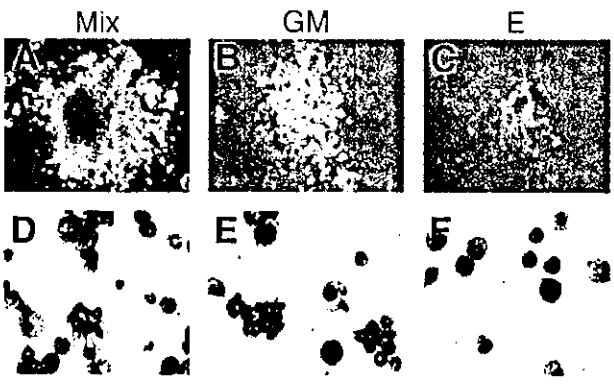

Figure 3. Colony formation of the rescued cells from *AML1*-deficient P-Sp. The hematopoietic defect of *AML1*-deficient P-Sp regions was rescued by retroviral expression of AML1b, and the rescued cells were plated into MethoCult3434 medium. The rescued cells generated various types of hematopoietic colonies including definitive origins. Representative hematopoietic colonies by 7 days of culture are shown. (A-C) Morphology of the colonies. (D-F) Cytospin preparation of corresponding cell populations. Cytospins were stained with Wright-Giemsa. Mix indicates mixed colony; GM, granulocyte/macrophage colony; and E, erythroid colony. Photographs were taken with a Nikon Eclipse TE2000-U (Nikon Sankei) at a magnification of × 100.

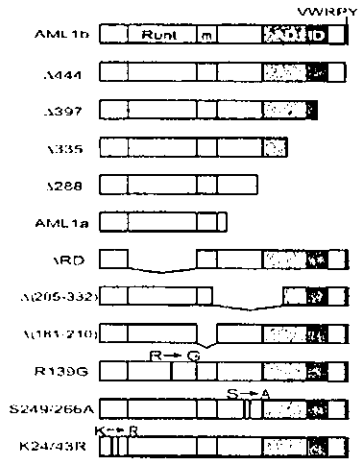

Figure 4. Structures of AML1 and its mutants. The structures of various AML1 mutants are presented schematically. Runt indicates the Runt domain; AD, *trans*-activation domain; ID, inhibitory domain; VWRPY, VWRPY motif; m, a binding region for mSin3A. R→G means a missense mutation at codon 139, which lead to a change of amino acid (R139G; single-letter amino acid code). S→A means a missense mutation at codon 249 and 266, which lead to changes of amino acids (S249A and S266A). K→R means a missense mutation at codon 24 and 43, which lead to changes of amino acid (K24R and K43R).

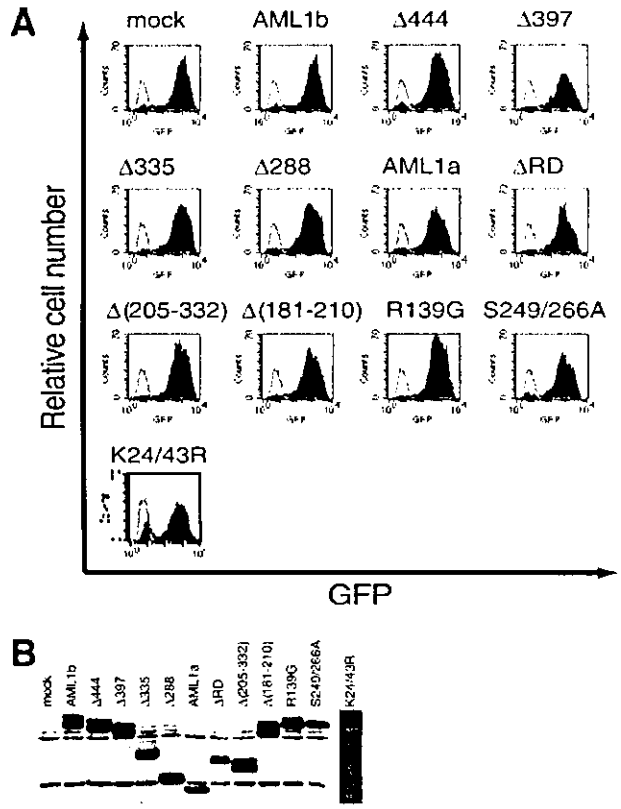

Figure 5. Infection efficiencies of retroviruses expressing AML1 or its mutants. (A) The efficiency of retrovirus-mediated gene transfer of AML1 or its mutants was estimated by infecting NIH3T3 cells. Retrovirus-infected cells were evaluated by the expression of GFP (shaded histograms). Also shown are the noninfected NIH3T3 cells (open histograms). All the retroviruses infected more than 80% of NIH3T3 cells. (B) Expression of AML1 or its mutant proteins in infected NIH3T3 cells. The expression is monitored by immunoblotting of whole-cell lysates with anti-AML1.

enhancement of the transcriptional activity. Finally, AML1b-K24/43R is an acetylation-defective mutant, in which the 2 lysine residues were substituted with arginines. Remarkably, all of these mutants retained the ability to rescue the hematopoietic defect in contrast to the mutants of the Runt domain (Figure 6H,J,K). The cells rescued by these AML1 mutants contained CFCs, expressed hematopoietic cell surface markers, and were morphologically indistinguishable from the rescued cells by wild-type AML1b (data not shown). From these findings, we concluded that the hematopoietic potential of AML1 does not require the interaction with mSin3A, ERK-dependent phosphorylation, or p300-mediated acetylation. Some posttranslational modifications, as well as repressor activities, of AML1 may not necessarily be required for early hematopoietic development. Given that all of these mutants retain a basal activity of gene transcription,[20,42,43] however, these results again argue a close correlation between the transcriptional activity of AML1 and its hematopoietic potential.

Runx2/AML3 and Runx3/AML2 have the capacity to rescue the hematopoietic defect of *AML1*-deficient P-Sp regions

In addition to AML1, there are 2 other known mammalian Runx transcription factors, Runx2/AML3 and Runx3/AML2. To determine whether these Runx proteins have the capacity to substitute for AML1 in hematopoiesis, we infected *AML1*-deficient P-Sp with retroviruses carrying Runx2/AML3 or Runx3/AML2. The infection efficiency and protein expression were assessed by the same method used for AML1 mutants (Figure 7A-B). Interestingly, enforced expression of either Runx2 or Runx3 in *AML1*-deficient P-Sp resulted in the generation of numerous hematopoietic cells (Figure 7C). There is no difference among the rescued hematopoietic cells by all 3 Runx proteins in terms of morphology, expression of surface markers, and CFC activity (data not shown). These results suggest redundant roles among Runx proteins in early hematopoietic development.

Discussion

The striking phenotype of *AML1*-deficient mice has demonstrated an essential role for AML1 in the formation of definitive hematopoiesis during development. However, domain contribution of AML1 in early hematopoietic development has not yet been fully elucidated. Here we described an assay for AML1 function based on the ability to rescue hematopoiesis from the *AML1*-deficient P-Sp regions. Using this system, we found that the hematopoietic potential of AML1 was closely related to its transcriptional activity. Among those mutants used in this study, AML1bΔ444, AML1bΔ397, and AML1bΔ(181-210) are transcriptionally active in a luciferase assay (Kurokawa et al[41]; data not shown). AML1b-S249/266A and AML1b-K24/43R also retain a basal activity of gene transcription. All of these transcriptionally active mutants of AML1 could confer hematopoietic activity on *AML1*-deficient P-Sp regions. On the contrary, other mutants that lose the transcriptional activation ability (Lutterbach et al,[20] Kurokawa et al[41]; data

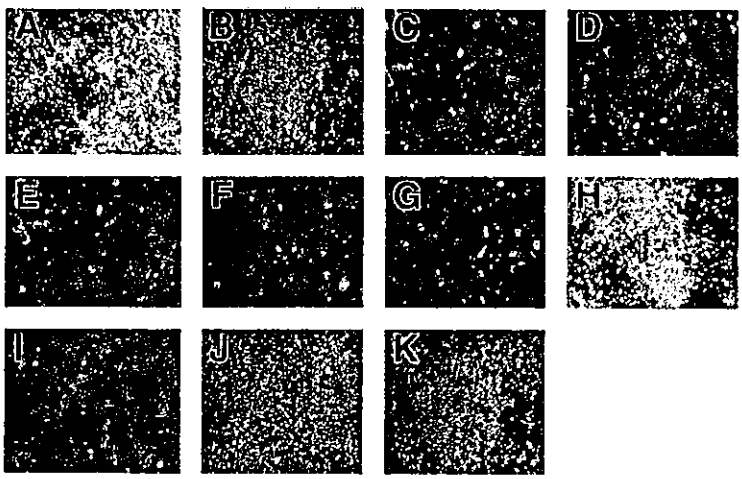

Figure 6. Hematopoietic potential of the AML1 mutants. Cells isolated from *AML1*-deficient P-Sp regions were infected with retrovirus containing the AML1 mutants. Each retrovirus contained (A) AML1bΔ444, (B) AML1bΔ397, (C) AML1bΔ335, (D) AML1bΔ288, (E) AML1a, (F) AML1bΔRD, (G) AML1bΔ(205-332), (H) AML1bΔ(181-210), (I) AML1b-R139G, (J) AML1b-S249/266A, or (K) AML1b-K24/43R. AML1bΔ444 (A), AML1bΔ397 (B), AML1bΔ(181-210) (H), AML1b-S249/266A (J), and AML1b-K24/43R (K) retain the ability to rescue the hematopoietic defect of *AML1*-deficient P-Sp regions, whereas other mutants do not. Shown are phase-contrast microscopic views of these cultures at 14 days. Photographs were taken with a Nikon Eclipse TE2000-U (Nikon Sankei) at a magnification of × 100.

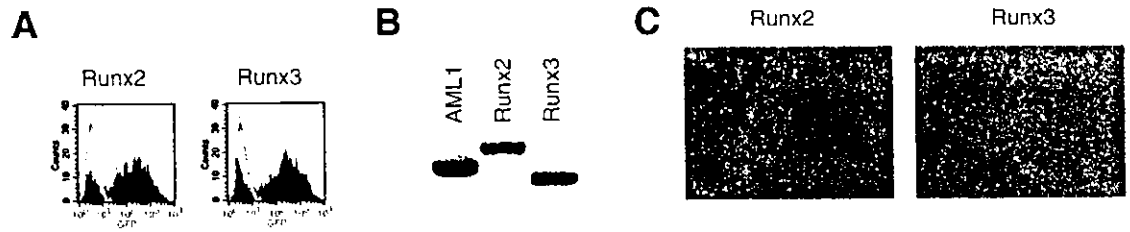

Figure 7. Runx2/AML3 and Runx3/AML2 have the capacity to rescue the hematopoietic defect of *AML1*-deficient P-Sp regions. (A) The efficiency of retrovirus-mediated gene transfer of Runx2/AML3 or Runx3/AML2 was estimated by infecting NIH3T3 cells. Retrovirus-infected cells were evaluated by the expression of GFP (shaded histograms). Also shown are the noninfected NIH3T3 cells (open histograms). (B) Expression of 3 Runx proteins (AML1, Runx2/AML3, and Runx3/AML2) in infected NIH3T3 cells. The expression is monitored by immunoblotting of whole-cell lysates with anti-Flag. (C) Both Runx2/AML3 and Runx3/AML2 have the capacity to rescue the hematopoietic defect of *AML1*-deficient P-Sp regions. Shown are phase-contrast microscopic views of these cultures at 14 days visualized using a Nikon Eclipse TE2000-U (Nikon Sankei) at a magnification of × 100.

not shown) did not rescue the hematopoietic defect. Previously, the C-terminal deletion mutants of AML1b were analyzed with the ES cell culture system. Among them, the mutants containing *trans*-activation subdomains retained the hematopoietic potential.[35] In the present study, we extended these analyses by examining various AML1 mutants and clearly demonstrated that the transcriptional activity of AML1 is essential for in vitro hematopoietic rescue of *AML1*-deficient P-Sp regions.

AML1 can also function as a transcriptional repressor depending on the target gene and the cellular context by recruiting corepressors, such as transduction-like enhancer of split (TLE) and mSin3A. Of these, TLE interacts with AML1 by recognizing its C-terminal VWRPY motif,[21-23] and mSin3A interacts mainly through the region between amino acids 181 and 210.[20] As shown in the current study, the deletion mutants of AML1 that do not interact with these corepressors retained the hematopoietic potential. Therefore, repressor activity of AML1 appears dispensable in early hematopoietic development. Recently, investigations using T-cell–specific *AML1*-deficient mice demonstrated that AML1 has critical functions during thymocyte development.[47] In addition, the *trans*-repression activity of AML1 was suggested to play a role in early thymocyte development.[36] Therefore, the function of AML1 as a transcriptional repressor should be important for appropriate T-cell differentiation. Because the culture system described here lacks the ability to support T-cell development, we are currently establishing another in vitro culture system to investigate the domain contribution of AML1 in T-cell development.

Although a genetic mutation of AML1 has been found in patients with hematologic malignancies,[12-14] the precise mechanisms of leukemogenesis caused by these mutations remain uncertain. Significant in this regard is our observation that AML1b-R139G, the AML1 mutant found in a MDS patient,[13] has lost the hematopoietic potential. This is the first direct evidence that the point mutation in the *AML1* gene, which was found in a patient with hematologic malignancy, leads to loss of its biologic activity in hematopoiesis. Taken together, this experimental system should contribute to further clarification of the molecular basis for leukemogenesis mediated by subtle mutations in the *AML1* gene.

Our study clearly demonstrated that both Runx2/AML3 and Runx3/AML2 have the capacity to rescue the hematopoietic defect of *AML1*-deficient P-Sp regions. Moreover, we also showed that "human" Runx proteins could substitute for the "murine" AML1 in early hematopoietic development because we used human cDNAs in this study. These results are consistent with the fact that the Runt and the *trans*-activation domains, which are essential for hematopoiesis, are highly conserved among members of mammalian Runx family. Thus, Runx-mediated hematopoietic activity depends on the evolutionarily conserved domains in Runx proteins.

In summary, we established an experimental culture system to efficiently examine the hematopoietic potential of Runx transcription factors. By analysis of the mutants, we precisely mapped the region responsible for the hematopoietic potential of AML1 and demonstrated that the transcriptional activity of AML1 is essential for early hematopoietic development. Furthermore, our results suggest a functional redundancy of mammalian Runx proteins in hematopoiesis.

Acknowledgments

We thank M. Ohki for the gift of the human AML1 cDNA, Y. Ito for the human Runx2/AML3 and Runx3/AML2 cDNAs, T. Kitamura for the Plat-E packaging cells and pMY/IRES-EGFP retrovirus vector, T. Nakano for the OP9 stromal cells, and Kirin Brewery Pharmaceutical Research Laboratory for cytokines.

References

1. Kania MA, Bonner AS, Duffy JB, Gergen JP. The Drosophila segmentation gene runt encodes a novel nuclear regulatory protein that is also expressed in the developing nervous system. Genes Dev. 1990;4:1701-1713.
2. Kagoshima H, Shigesada K, Satake M, et al. The Runt domain identifies a new family of heteromeric transcriptional regulators. Trends Genet. 1993;9:338-341.
3. Ogawa E, Maruyama M, Kagoshima H, et al. PEBP2/PEA2 represents a family of transcription factors homologous to the products of the Drosophila runt gene and the human AML1 gene. Proc Natl Acad Sci U S A. 1993;90:6859-6863.
4. Wang S, Wang Q, Crute BE, Melnikova IN, Keller SR, Speck NA. Cloning and characterization of subunits of the T-cell receptor and murine leukemia virus enhancer core-binding factor. Mol Cell Biol. 1993;13:3324-3339.
5. Sasaki K, Yagi H, Bronson RT, et al. Absence of fetal liver hematopoiesis in mice deficient in transcriptional coactivator core binding factor beta. Proc Natl Acad Sci U S A. 1996;93:12359-12363.
6. Wang Q, Stacy T, Miller JD, et al. The CBFbeta subunit is essential for CBFalpha2 (AML1) function in vivo. Cell. 1996;87:697-708.
7. Niki M, Okada H, Takano H, et al. Hematopoiesis in the fetal liver is impaired by targeted mutagenesis of a gene encoding a non-DNA binding subunit of the transcription factor, polyomavirus enhancer binding protein 2/core binding factor. Proc Natl Acad Sci U S A. 1997;94:5697-5702.
8. Miyoshi H, Shimizu K, Kozu T, Maseki N, Kaneko Y, Ohki M. t(8;21) breakpoints on chromosome 21 in acute myeloid leukemia are clustered within a limited region of a single gene, AML1. Proc Natl Acad Sci U S A. 1991;88:10431-10434.
9. Ohki M. Molecular basis of the t(8;21) translocation in acute myeloid leukaemia. Semin Cancer Biol. 1993;4:369-375.
10. Look AT. Oncogenic transcription factors in the human acute leukemias. Science. 1997;278: 1059-1064.
11. Kurokawa M, Hirai H. Role of AML1/Runx1 in the pathogenesis of hematological malignancies. Cancer Sci. 2003;94:841-846.
12. Osato M, Yanagida M, Shigesada K, Ito Y. Point mutations of the RUNx1/AML1 gene in sporadic and familial myeloid leukemias. Int J Hematol. 2001;74:245-251.
13. Imai Y, Kurokawa M, Izutsu K, et al. Mutations of

the AML1 gene in myelodysplastic syndrome and their functional implications in leukemogenesis. Blood. 2000;96:3154-3160.

14. Harada H, Harada Y, Niimi H, Kyo T, Kimura A, Inaba T. High incidence of somatic mutations in the AML1/RUNX1 gene in myelodysplastic syndrome and low blast percentage myeloid leukemia with myelodysplasia. Blood. 2004;103:2316-2324.
15. Okuda T, van Deursen J, Hiebert SW, Grosveld G, Downing JR. AML1, the target of multiple chromosomal translocations in human leukemia, is essential for normal fetal liver hematopoiesis. Cell. 1996;84:321-330.
16. Wang Q, Stacy T, Binder M, Marin-Padilla M, Sharpe AH, Speck NA. Disruption of the Cbfa2 gene causes necrosis and hemorrhaging in the central nervous system and blocks definitive hematopoiesis. Proc Natl Acad Sci U S A. 1996;93:3444-3449.
17. Miyoshi H, Ohira M, Shimizu K, et al. Alternative splicing and genomic structure of the AML1 gene involved in acute myeloid leukemia. Nucleic Acids Res. 1995;23:2762-2769.
18. Kanno T, Kanno Y, Chen LF, Ogawa E, Kim WY, Ito Y. Intrinsic transcriptional activation-inhibition domains of the polyomavirus enhancer binding protein 2/core binding factor alpha subunit revealed in the presence of the beta subunit. Mol Cell Biol. 1998;18:2444-2454.
19. Kitabayashi I, Yokoyama A, Shimizu K, Ohki M. Interaction and functional cooperation of the leukemia-associated factors AML1 and p300 in myeloid cell differentiation. EMBO J. 1998;17:2994-3004.
20. Lutterbach B, Westendorf JJ, Linggi B, Isaac S, Seto E, Hiebert SW. A mechanism of repression by acute myeloid leukemia-1, the target of multiple chromosomal translocations in acute leukemia. J Biol Chem. 2000;275:651-656.
21. Aronson BD, Fisher AL, Blechman K, Caudy M, Gergen JP. Groucho-dependent and -independent repression activities of Runt domain proteins. Mol Cell Biol. 1997;17:5581-5587.
22. Imai Y, Kurokawa M, Tanaka K, et al. TLE, the human homolog of groucho, interacts with AML1 and acts as a repressor of AML1-induced transactivation. Biochem Biophys Res Commun. 1998;252:582-589.
23. Levanon D, Goldstein RE, Bernstein Y, et al. Transcriptional repression by AML1 and LEF-1 is mediated by the TLE/Groucho corepressors. Proc Natl Acad Sci U S A. 1998;95:11590-11595.
24. Orkin SH. Development of the hematopoietic system. Curr Opin Genet Dev. 1996;6:597-602.
25. Godin IE, Garcia-Porrero JA, Coutinho A, Dieterlen-Lievre F, Marcos MA. Para-aortic splanchnopleura from early mouse embryos contains B1a cell progenitors. Nature. 1993;364:67-70.
26. Cumano A, Dieterlen-Lievre F, Godin I. Lymphoid potential, probed before circulation in mouse, is restricted to caudal intraembryonic splanchnopleura. Cell. 1996;86:907-916.
27. Muller AM, Medvinsky A, Strouboulis J, Grosveld F, Dzierzak E. Development of hematopoietic stem cell activity in the mouse embryo. Immunity. 1994;1:291-301.
28. Medvinsky A, Dzierzak E. Definitive hematopoiesis is autonomously initiated by the AGM region. Cell. 1996;86:897-906.
29. North T, Gu TL, Stacy T, et al. Cbfa2 is required for the formation of intra-aortic hematopoietic clusters. Development. 1999;126:2563-2575.
30. North TE, de Bruijn MF, Stacy T, et al. Runx1 expression marks long-term repopulating hematopoietic stem cells in the midgestation mouse embryo. Immunity. 2002;16:661-672.
31. de Bruijn MF, Speck NA, Peeters MC, Dzierzak E. Definitive hematopoietic stem cells first develop within the major arterial regions of the mouse embryo. EMBO J. 2000;19:2465-2474.
32. Yokomizo T, Ogawa M, Osato M, et al. Requirement of Runx1/AML1/PEBP2alphaB for the generation of haematopoietic cells from endothelial cells. Genes Cells. 2001;6:13-23.
33. Mukouyama Y, Hara T, Xu M, et al. In vitro expansion of murine multipotential hematopoietic progenitors from the embryonic aorta-gonad-mesonephros region. Immunity. 1998;8:105-114.
34. Takakura N, Watanabe T, Suenobu S, et al. A role for hematopoietic stem cells in promoting angiogenesis. Cell. 2000;102:199-209.
35. Okuda T, Takeda K, Fujita Y, et al. Biological characteristics of the leukemia-associated transcriptional factor AML1 disclosed by hematopoietic rescue of AML1-deficient embryonic stem cells by using a knock-in strategy. Mol Cell Biol. 2000;20:319-328.
36. Nishimura M, Fukushima-Nakase Y, Fujita Y, et al. VWRPY motif-dependent and -independent roles of AML1/Runx1 transcription factor in murine hematopoietic development. Blood. 2004;103:562-570.
37. Nakano T, Kodama H, Honjo T. Generation of lymphohematopoietic cells from embryonic stem cells in culture. Science. 1994;265:1098-1101.
38. Ichikawa M, Asai T, Saito T, et al. AML-1 is required for megakaryocytic maturation and lymphocytic differentiation, but not for maintenance of hematopoietic stem cells in adult hematopoiesis. Nat Med. 2004;10:299-304.
39. Kumano K, Chiba S, Kunisato A, et al. Notch1 but not Notch2 is essential for generating hematopoietic stem cells from endothelial cells. Immunity. 2003;18:699-711.
40. Kitamura T, Koshino Y, Shibata F, et al. Retrovirus-mediated gene transfer and expression cloning: powerful tools in functional genomics. Exp Hematol. 2003;31:1007-1014.
41. Kurokawa M, Tanaka T, Tanaka K, et al. Overexpression of the AML1 proto-oncoprotein in NIH3T3 cells leads to neoplastic transformation depending on the DNA-binding and transactivational potencies. Oncogene. 1996;12:883-892.
42. Tanaka T, Kurokawa M, Ueki K, et al. The extracellular signal-regulated kinase pathway phosphorylates AML1, an acute myeloid leukemia gene product, and potentially regulates its transactivation ability. Mol Cell Biol. 1996;16:3967-3979.
43. Yamaguchi Y, Kurokawa M, Imai Y, et al. AML1 is functionally regulated through p300-mediated acetylation on specific lysine residues. J Biol Chem. 2004;279:15630-15638.
44. Morita S, Kojima T, Kitamura T. Plat-E: an efficient and stable system for transient packaging of retroviruses. Gene Ther. 2000;7:1063-1066.
45. Mukouyama Y, Chiba N, Hara T, et al. The AML1 transcription factor functions to develop and maintain hematogenic precursor cells in the embryonic aorta-gonad-mesonephros region. Dev Biol. 2000;220:27-36.
46. Imai Y, Kurokawa M, Yamaguchi Y, et al. The corepressor mSin3A regulates phosphorylation-induced activation, intranuclear location, and stability of AML1. Mol Cell Biol. 2004;24:1033-1043.
47. Taniuchi I, Osato M, Egawa T, et al. Differential requirements for Runx proteins in CD4 repression and epigenetic silencing during T lymphocyte development. Cell. 2002;111:621-633.

MOLECULAR AND CELLULAR BIOLOGY, Feb. 2004, p. 1033–1043 Vol. 24, No. 3
0270-7306/04/$08.00+0 DOI: 10.1128/MCB.24.3.1033–1043.2004

The Corepressor mSin3A Regulates Phosphorylation-Induced Activation, Intranuclear Location, and Stability of AML1

Yoichi Imai,[1] Mineo Kurokawa,[1]* Yuko Yamaguchi,[1] Koji Izutsu,[1] Eriko Nitta,[1] Kinuko Mitani,[2] Masanobu Satake,[3] Tetsuo Noda,[4] Yoshiaki Ito,[5] and Hisamaru Hirai[1]

Department of Hematology and Oncology, Graduate School of Medicine, University of Tokyo, Bunkyo-ku, Tokyo 113-8655,[1] Department of Hematology, Dokkyo University School of Medicine, Tochigi 321-0207,[2] Department of Molecular Immunology, Institute of Development, Aging, and Cancer, Tohoku University, Sendai 980-0872,[3] and Department of Cell Biology, The Cancer Institute, Japanese Foundation for Cancer Research, Tokyo 170-0012,[4] Japan, and Institute of Molecular and Cell Biology, National University of Singapore, Singapore 117609, Singapore[5]

Received 17 March 2003/Returned for modification 8 May 2003/Accepted 31 October 2003

The *AML1* (*RUNX1*) gene, one of the most frequent targets of translocations associated with human leukemias, encodes a DNA-binding protein that plays pivotal roles in myeloid differentiation through transcriptional regulation of various genes. Previously, we reported that AML1 is phosphorylated on two serine residues with dependence on activation of extracellular signal-regulated kinase, which positively regulates the transcriptional activity of AML1. Here, we demonstrate that the interaction between AML1 and the corepressor mSin3A is regulated by phosphorylation of AML1 and that release of AML1 from mSin3A induced by phosphorylation activates its transcriptional activity. Furthermore, phosphorylation of AML1 regulates its intranuclear location and disrupts colocalization of AML1 with mSin3A in the nuclear matrix. PEBP2β/CBFβ, a heterodimeric partner of AML1, was shown to play a role in protecting AML1 from proteasome-mediated degradation. We show that mSin3A also protects AML1 from proteasome-mediated degradation and that phosphorylation-induced release of AML1 from mSin3A results in degradation of AML1 in a time-dependent manner. This study provides a novel regulatory mechanism for the function of transcription factors mediated by protein modification and interaction with cofactors.

AML1 (*RUNX1*) was first identified on chromosome 21 as the gene that is disrupted in the (8;21)(q22;q22) translocation, which is one of the most frequent chromosome abnormalities associated with acute myelogenous leukemia (AML) (20, 24, 29). *AML1* is also disrupted in t(3;21)(q26;q22), which is found in the blastic crisis phase of chronic myelogenous leukemia (23). It was also reported that the *AML1* gene is rearranged in acute lymphoblastic leukemia carrying t(12;21)(p12;q22) and that this translocation generates the TEL-AML1 fusion protein (5, 34). Furthermore, point mutations in the Runt domain of the *AML1* gene were found in patients with AML (31, 33), familial platelet disorder with predisposition to AML (35), or myelodysplastic syndrome (9). These findings suggest that the structural alterations of AML1 caused by translocations or point mutations trigger leukemic transformation of hematopoietic cells.

AML1 regulates the transcription of various genes that are important in hematopoiesis (27, 36, 37, 48). Furthermore, it has been revealed that AML1 can cause neoplastic transformation when overexpressed in fibroblasts, suggesting a potential role for AML1 in promoting cellular proliferation (17). From analyses of mice lacking *AML1*, it was shown that AML1 plays an important role in liver-derived hematopoiesis and angiogenesis (30, 38).

Previously, the regulatory mode of AML1 functions through signal transduction pathways was investigated, and it was revealed that AML1 is phosphorylated with dependence on the activation of extracellular signal-regulated kinase (ERK) (40). ERK-dependent phosphorylation enhances the transcriptional activity of AML1, and mutations of the phosphorylation sites reduce the transforming capacity of AML1 in fibroblasts (40). These results indicate that the functions of AML1 are potentially regulated by ERK-induced phosphorylation, which is activated by cytokine and growth factor stimuli. However, the mechanism by which the transcriptional ability of AML1 is activated by phosphorylation has not been clear.

A growing number of proteins have been shown to interact with AML1 to modify its function (2, 10, 12, 19, 21, 28, 44). Here, we have investigated whether these protein-protein interactions are affected by phosphorylation of AML1, and we found that the corepressor mSin3A is released from phosphorylated AML1, whereby the transcriptional activity of phosphorylated AML1 is activated. Furthermore, we demonstrated that mSin3A is a key regulator for the intranuclear localization and stability of AML1. This study reveals a previously unappreciated role of the corepressor mSin3A as a regulator of AML1.

MATERIALS AND METHODS

Plasmid construction. The pME-AML1, pME-PEBP2β, pCMV-MK, and Tww-tk-Luc reporter plasmids were constructed as described previously (41). The AML1 mutants S249/266A and S249/266E were obtained by replacing the serine residues with alanines or glutamic acids by the site-directed mutagenesis method for AML1 cDNA (15). FLAG-tagged AML1 constructs were generated as described previously (10). The deletion mutant of S249/266A, Δ(181-210)SA,

* Corresponding author. Mailing address: Department of Hematology and Oncology, Graduate School of Medicine, University of Tokyo, 7-3-1 Hongo, Bunkyo-ku, Tokyo 113-8655, Japan. Phone: 81-3-38150-5411, ext. 33118. Fax: 81-3-3815-8350. E-mail: kurokawa-tky@umin.ac.jp.